Cornell University
College of Engineering

Sibley School of Mechanical and Aerospace Engineering

Mason Peck
Assistant Professor
Mechanical & Aerospace Engineering
Cornell University
212 Upson Hall
Ithaca, NY 14853

Telephone: 607 255-4023
Fax: 607 255-1222
E-mail: mp336@cornell.edu

May 1, 2006

Dr. Robert A. Cassanova
Director, NIAC
75 5th Street N.W.
Suite 318
Atlanta, GA 30318

Dear Dr. Cassanova:

The attached report describes the results of our NIAC Phase I project, *Lorentz-Actuated Orbits: Electrodynamic Propulsion without a Tether*. Our experience has been a fascinating, and I think fruitful, exploration of some exciting new possibilities. You will receive a proposal for a Phase II effort soon.

We are deeply grateful for NIAC's sponsorship and hope that this report exceeds your expectations.

Sincerely,

Mason Peck

Principal Investigator
Space Systems Design Studio

Assistant Professor
Cornell University
Mechanical and Aerospace Engineering

Contents

Tables

Figures

Lorentz-Actuated Orbits: Electrodynamic Propulsion without a Tether
Final Report

1. Abstract

The NIAC Phase I investigation described here explores the concept of using the Lorentz force as a revolutionary means of accelerating a spacecraft. This force acts on a charged particle moving in a magnetic field, as in the case of a satellite carrying a biased electrical charge and orbiting within a planetary or stellar magnetosphere. This propellantless propulsion technique may represent the last area of classical physics that has not yet been considered for spaceflight dynamics. A spacecraft mission whose architecture is based on the Lorentz-Actuated Orbit benefits from propellantless, non-Keplerian orbits: for example,

- orbit planes that precess synchronously with the planet's rotation, but at lower altitudes than the classical geostationary solution
- Earth and solar escape (elliptical to hyperbolic orbits) and planetary capture (hyperbolic to elliptical)
- swarms of spacecraft that hover in non-Keplerian orbits, such as a formation of radially positioned vehicles with constant angular velocity at different altitudes
- rendezvous along the velocity direction, with no need for orbit raising and lowering
- orbits whose lines of apsides rotate synchronously with the planet, its moon, or the sun, offering continuous lunar free-return trajectories and lunar resupply possibilities
- low-earth orbits that experience neither cumulative atmospheric drag nor J2 perturbations

The Phase I studyh mapped out the heretofore unexplored, coupled dynamics of familiar celestial mechanics and cyclotron-style motion of a charged particle in a magnetic field and discovered a number of new system architectures for space travel. We identified areas of technology advancement required for this system to be feasible and compared this concept to existing methods of propulsion in terms of key metrics: mass, power, cost, time of flight, and risk. Future efforts will focus on the feasibility issues by evaluating these low-TRL technologies to a point where Lorentz-actuated orbits can be considered for a future NASA mission. Our goals for a future phase are the following:

- Develop and exercise the algorithms and modeling tools required to understand spacecraft capable of experiencing a Lorentz-Actuated Orbit, including NASCAP and other in-house developed software for evaluating the coupled behaviors of spaceborne-plasma charging and orbit dynamics.
- Identify the lowest-risk charge-storage subsystem (i.e. capacitor) from among the technologies identified in the Phase I effort and detail its performance in the space environment, with an emphasis on plasma interactions.
- Demonstrate and characterize the self-capacitance for the case of a scaled test in a representative plasma environment.
- Identify the lowest-risk charge-maintenance subsystem (i.e. charged-particle source and related components) from among the technologies identified in the Phase I effort and detail its performance in the space environment, with an emphasis on plasma interactions
- Devise a promising, candidate mission architecture in an effort to identify and tie up loose ends that would otherwise represent unacceptable risk to a NASA application.

2. Introduction

This NIAC Phase I study evaluates the use of the Lorentz force as a revolutionary means of accelerating a spacecraft. To state our project more precisely, we have undertaken a study of the unexplored, coupled dynamics of familiar celestial mechanics and cyclotron-style motion of a charged particle in a magnetic field for the purpose of realizing new system architectures for space travel. In this project, we seek to identify the technology-advancement needs that will enable these architectures. A key outcome of the project is a comparison of the proposed concept to existing methods of propulsion in terms of key metrics: mass, power, cost, and risk.

Figure 1 shows a particular implementation of this concept. In this scenario, a spherical self-capacitor holds electrical charge at some potential relative to the surrounding plasma. As the spacecraft travels at some velocity relative to the magnetic field, the Lorentz force it feels accelerates it, ultimately toward earth escape. The details are subtle and include important effects due to the rotating earth and interactions with the plasma environment.

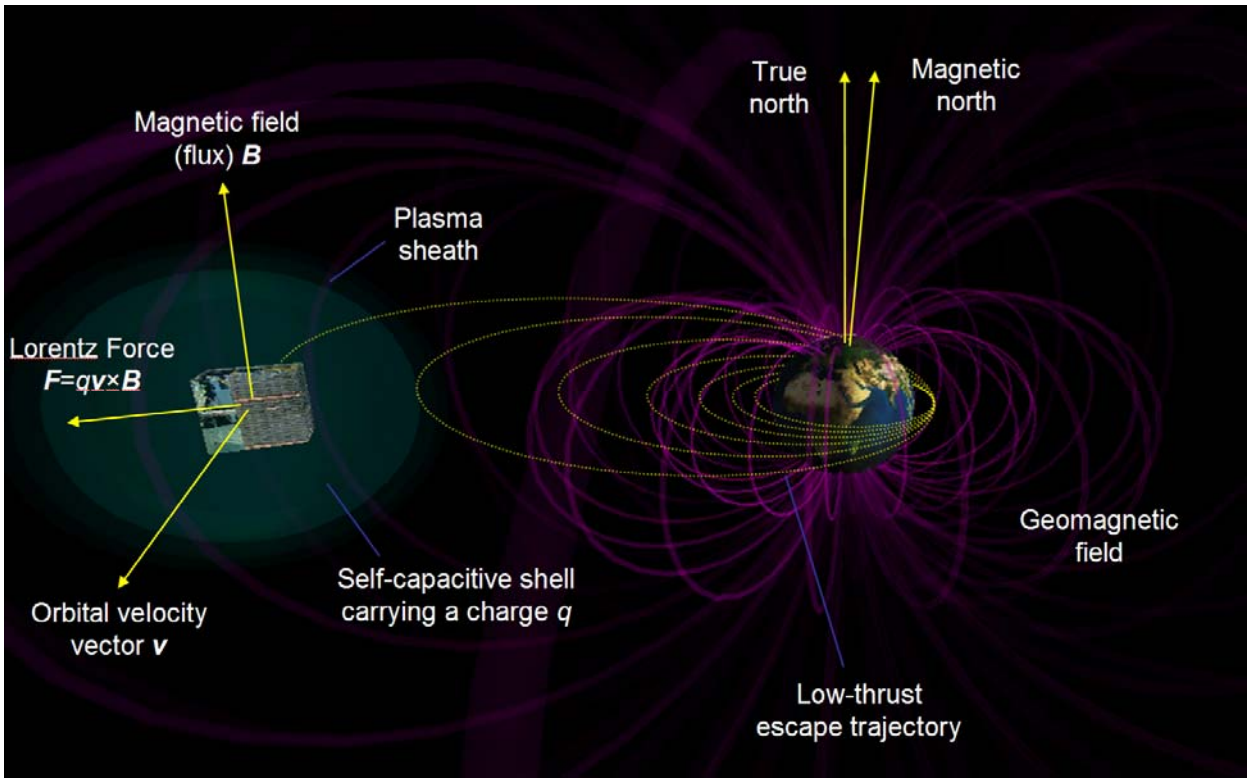

Figure 1. LAO Concept Realized as a Spacecraft with a Capacitive Faraday-Cage Shell Providing Lorentz Force for Earth Escape

The fundamental principles at work here are well understood and have been since the 19th century. Less well developed are the technologies that enable a spacecraft architecture of this kind to be realized. The prospect of propellantless space flight alone is a powerful motivator for developing these technologies. But an even greater motivation can be found the broad range of applications beyond earth escape. This report describes many applications and provides thoroughly detailed, and new, analytical results that allow these applications to be evaluated in terms of cost, risk, and performance.

Far from narrowing the applicability of the LAO concept, the Phase I work led to the discovery of surprising new applications and pointed the way toward engineering solutions to the problems of creating and maintaining a biased electrical charge. Even during the last few months, our effort to consider the LAO without preconceived notions has proved very fruitful. This proposal summarizes these results and describes the next step in bringing this revolutionary, futuristic concept closer to the present.

3. Physics and Experimental Background

First, let us be clear about what the Lorentz-Actuated Orbit (LAO) is not. An LAO does not involve the use of electrodynamic tethers, although the physics is related. By contrast, an LAO-capable spacecraft may be very compact. The charge it carries travels at perhaps thousands of meters per second relative to the geomagnetic field (much faster than the electrons in a tether). This moving charge results in a force similar to what a tether experiences, but the LAO spacecraft offers a far more mass-efficient design. Also, an LAO does not work though electrostatic levitation. That is, an LAO does not depend on Coulomb forces that may act on the charged spacecraft. Power is required—we do not claim to get something for nothing—but only enough to establish and maintain a high electrical potential on part of the spacecraft.

A particle that carries an electrical charge q with a velocity $\boldsymbol{v}$ relative to a magnetic field $\boldsymbol{B}$ experiences the Lorentz force $\boldsymbol{F}_{\mathrm{L}}$:

$$\boldsymbol{F}_L = q\boldsymbol{v} \times \boldsymbol{B} \tag{1}$$

A consequence of relativistic electrodynamics, this force is used as a means of steering the electron beam in a cathode-ray tube and, confirmed by data gathered at Jupiter and Saturn during the past two decades, has been shown to govern the orbital dynamics of dust in planetary rings. In fact, the most in-depth treatment of LAO celestial mechanics is found in the work of Schaffer, Burns, et al. on planetary dusty plasmas[1,2]. Their work offers explanations for gaps in Jupiter's and Saturn's rings that are based on identifying resonances in the orbit dynamics. The resonances arise thanks to interactions among gravity and small effects such as solar pressure, lunar perturbations, and the Lorentz force. The success of these studies validates models of particle charging and demonstrates that the Lorentz force leads to non-Keplerian orbits, at least for micron-size particles at a few Volts of potential. Dusty plasma researchers have also considered the problem of dust grains in orbit, but with a primary interest in plasmadynamics rather than celestial mechanics[3]. Figure 2 shows a focused beam of electrons traveling in a circular path due to the Lorentz force that acts on them in the presence of a magnetic field generated by Helmholtz coils.

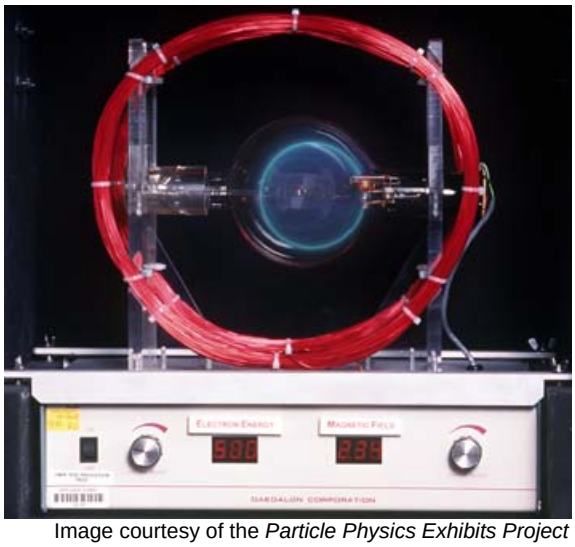

Image courtesy of the *Particle Physics Exhibits Project*

Figure 2. Electron beam diverted by the Lorentz Force

The literature on spacecraft charging is extensive. Much of it is concerned with the deleterious effects of differential charge, a problem that arises when dissimilar or discontinuous materials acquire potential as the spacecraft travels through the space plasma[4]. The photoelectric effect, in which photons cause some materials to emit electrons, can also be responsible. These potentials can result in arcing from one component to another or sputtering of surfaces and are to be avoided, whether by the choice of materials, charge management (by grounding to the surrounding plasma), or by careful placement of components and incorporation of Faraday cages[5,6]. These studies are concerned primarily with predicting charge levels and assessing the risks of material damage due to interactions with the natural environment. By contrast, we consider the active application of charge to a spacecraft body; and although the influence of the plasma is very relevant for the design LAO capable spacecraft, the equilibrium potentials achieved passively are not of direct interest here.

Another class of studies on spacecraft charging stems from ballistic missile defense research during the past two decades, much of it for the Strategic Defense Initiative of the 1980s. This work has involved high-energy ion and electron beam emission from sounding rockets and spacecraft. Some examples of rocket platforms include the Beam Experiment Aboard Rocket (BEAR), Space Power Experiment Aboard Rockets (SPEAR) I through III[7,8], and MAIMIK[9]. Satellite-based experiments include the high-altitude Application Technology Satellite 6 (ATS-6) and Spacecraft Charging at High Altitude (SCATHA) satellites. Theoretical studies have also been undertaken[10,11]. Some of the results of these studies are used in the analysis below. The Space Shuttle has also been the subject of charging studies, for example during the 1992 flight of the Tethered Satellite System (TSS)[12].

Augmented with the Lorentz Force, Newton's law of gravitation for a particle of mass m moving in the r^{-2} gravitational field of a point mass M becomes

$$m\frac{{}^{N}d^{2}}{dt^{2}}\boldsymbol{r} = -m\frac{\mu}{r^{2}}\hat{\boldsymbol{r}} + q\left(\frac{{}^{N}d}{dt}\boldsymbol{r} - \boldsymbol{\omega}_{e}\times\boldsymbol{r}\right)\times\boldsymbol{B} \qquad (2)$$

where the superscript N indicates a derivative taken with respect to a Newtonian, or inertial, frame, $\boldsymbol{r}$ is the vector position (magnitude r and direction $\hat{\boldsymbol{r}}$) of the particle relative to the system

barycenter, $\mu = MG$ where G is the universal gravitational constant, q is the electric charge on the particle, $\boldsymbol{\omega}_e$ is the earth's angular velocity vector (herafter taken to be constant in N), and $\boldsymbol{B}$ is the magnetic field vector. This expression acknowledges that it is the particle's velocity relative to the magnetic field $\boldsymbol{v} = \frac{{}^{N}d}{dt}\boldsymbol{r} - \boldsymbol{\omega}_e \times \boldsymbol{r}$ that determines the Lorentz force. In the simplest model, the earth's magnetic field rotates with the earth. By relativity, this time-varying magnetic field represents an electric field, which is the means by which work can be done on the LAO.

In a frame E that rotates with the earth, the acceleration in terms of the relative velocity $\boldsymbol{v} = \frac{{}^{E}d}{dt}\boldsymbol{r}$ and a gravitational potential Φ_{gr} is

$$\frac{{}^{E}d}{dt}\boldsymbol{v} = -\nabla\Phi_{gr} + \frac{q}{m}\boldsymbol{v} \times \boldsymbol{B} - 2\boldsymbol{\omega}_e \times \boldsymbol{v} - 2\boldsymbol{\omega}_e \times \left(\boldsymbol{\omega}_e \times \boldsymbol{r}\right), \tag{3}$$

where dividing through by m introduces the commonly used charge per mass q/m as a parameter that determines the scale of the Lorentz force.

This result confirms that a magnetic field does no work in a frame where the magnetic field is constant. However, the geomagnetic field's rotation in an inertial frame, due to the earth's motion, induces a so-called co-rotational electric field that leads to time-varying energy. In exploiting this principle for propulsion, the spacecraft steals a little kinetic energy from the planet's rotation, like a flyby alters the orbital energy of the body it passes.

These relatively few equations give rise to many special solutions, some of which are summarized below. The appendices provide considerable detail on these derivations. What's revolutionary is the prospect of non-Keplerian orbits, requiring no propellant, but with a compact spacecraft structure. In fact, most LAOs exhibit time-varying orbital elements. With an LAO, no longer would a spacecraft mission be limited to fixed conic sections or the tradeoff of dynamic orbits vs. propellant expenditure. Instead, the natural behaviors we have identified for LAO spacecraft vary with relatively little control effort, leading to never-before considered missions, as Section 4.1 explains.

Several technologies enable an LAO-capable spacecraft. First, the spacecraft must exhibit significant self-capacitance, the property that allows a body to maintain some electrical (or electrostatic charge) when it is raised to an electrical potential. Conductive spheres, such as are found on Vandegraaff generators, are familiar examples of self-capacitive bodies. Second, because of the fundamental physical law of conservation of charge, the spacecraft must be able to inject charge into the environment as a means to adjust the charge it carries. Plasma contactors, electron and ion beams, pyroelectric crystals, and alpha-particle emitting isotopes can provide such a function. The first two even offer space heritage. Third, the spacecraft's interactions with the plasma environment can be either beneficial or detrimental, but managing them to minimize power required is a critical function for the spacecraft design. Finally, an LAO spacecraft takes advantage of compact charge-storage devices to allow much higher-agility attitude dynamics than solar sails and tethers, both of which suffer from the difficulty in keeping their large structures aligned with the directions necessary for thrust.

4. Results from the Phase I Study

Our NIAC Phase I effort resulted in several important discoveries. They are described here in terms of three main areas: mission architectures, enabling technologies, and performance comparisons. Our initial assessment of the LAO concept addressed all three areas, analyzing strategies for holding onto the requisite charge and powering the spacecraft, developing analytical tools and basic results for plasma interactions, and drafting a technology roadmap to support the many mission concepts we have identified. While we learned a great deal, all elements of this early analysis underscored for us the need for experimental investigation to complement our analytical work. We even extended the scope of the Phase I study to include some preliminary experimentation, but more remains to be done to raise the Technology Readiness Level (TRL) of the LAO concept.

4.1 Mission Architectures

Our Phase I research is not merely a study of a narrowly applied, single technology. Instead, our research exploits the fundamental physics and mathematical results to arrive at spacecraft system concepts, which are described qualitatively here. In general, the proposed propulsion concept allows freight and passengers to be transported throughout the solar system, using planetary magnetic fields as stepping stones. It also enables science missions that have never before been considered.

This study will explore the validity of this concept for spacecraft propulsion within the larger context of NASA's robotic and human missions in the next several decades. Our preliminary investigations suggest that existing technologies can be used to realize modest, though meaningful, ΔV. For transportation of bulk materials and passengers throughout the solar system, the technology for high-capacitance spacecraft must move beyond what is available today.

Propellantless Earth-to-Gas-Giant Mission: q/m *between 0.1 and 1.0 C/kg*

As the spacecraft orbits a planet, the co-rotational electrical field (associated with the rotating planetary magnetic field) does mechanical work, increasing or decreasing the orbit's semimajor axis. The rate of change is given by

$$\dot{a} = -\frac{qB}{m}\frac{2a^2}{\mu}\dot{r}r\omega_e . \tag{3}$$

For the greatest effect, the spacecraft's charge is modulated so that it is high for half the orbit (true anomaly 0^o – 180^o) and low (or negative) for the other half. This bang-bang control scheme is optimal in the case where the LAO-capable spacecraft can achieve a certain maximum charge. Departing the earth in this fashion from an initial Geostationary Transfer Orbit can be done without propellant. Reversing the earth-escape control modulation enables the spacecraft to slow down upon reaching, say, Jupiter. In fact, Jupiter's very high magnetic field and high spin rate make it ideal for this application. Executing typical Jupiter capture maneuver with an LAO would save propellant and would offer a means of making the maneuver plan more forgiving of navigation errors.

In a traditional flyby, a spacecraft takes on a little of the planet's angular momentum about the sun as it passes. In the LAO analogue, the spacecraft steals a little of the planet's angular momentum about its mass center (not about the sun). A combined traditional and LAO flyby could offer the greatest benefit, reducing the time from earth to the gas giant.

Appendix B of this report is a draft of our paper on this subject, which will also be presented at the 2006 AIAA GNC Conference.

V-bar Rendezvous: q/m *between 0.001 and 0.01 C/kg*

One rarely considers gravitational potential as a tunable parameter for spacecraft. However, the Lorentz-force effect can work against gravity in a way that makes spacecraft behave as if the Earth were more or less massive than it really is. There are likely more applications than we have identified to date.

A circular LAO may exhibit an orbital angular velocity (mean motion) that differs from that of a Keplerian orbit of the same radius. This angular velocity is given by

$$\omega = -\frac{q}{m} B_0 \frac{r_0^3}{r^3} \pm \frac{\sqrt{\left(\frac{q}{m} B_0 r_0^3\right)^2 + 4r^3\left(\mu + \frac{q}{m}\omega_e B_0 r_0^3\right)}}{2r^3}. \tag{3}$$

The obvious application of this principle is a spacecraft that can rendezvous with another without the use of propellant. The contamination risks and complexity associated with discontinuous, impulsive maneuvers are absent here. The basic principle can be extended to elliptical orbits, a task we hope to undertake in the next phase of this work. The Vision for Space Exploration includes many such maneuvers, e.g. for in-orbit servicing, assembly in orbit, and transfer of passengers and cargo among various vehicles. The clear relevance of this single application is a powerful argument for pursuing LAO technology.

Constant Formation with Radial Relative Positions: q/m *between 0.0001 and 0.01 C/kg*

Formation-flying satellites with traditional propulsion can achieve only certain very limited shapes. For example NASA's Magnetospheric Multiscale Mission uses a tetrahedron of spacecraft, but this arrangement is only achievable at certain points in the orbit. However, using the Lorentz force opens up far more possibilities. In the case of a tetrahedron, a rotating formation of this shape can be realized throughout the entire orbit using the Lorentz force to adjust the mean motion of spacecraft at varying distances. LAO-capable spacecraft can fly with the same orbital period at varying radii:

$$r = \sqrt[3]{\frac{1}{\omega^2}\left(\mu - \frac{q}{m}(\omega - \omega_e) B_0 r_0^3\right)} \tag{4}$$

These formations can also achieve surprising shapes, some that are clearly impossible with Keplerian orbits and practical propellant usage. Mr. Brett Streetman, a doctoral student at Cornell, is working on this topic as part of his dissertation.

Geosynchronous Low-Earth Orbits: q/m *between 1.0 and 2.9 C/kg*

Mr. Streetman, on our research team, has discovered one of the more remarkable LAOs. It is one in which the orbit precesses about the magnetic pole in a direction determined by the charge's polarity. Figure 3 shows the relevant vectors. In summary, a constant charge (no modulation necessary) results in a constant precession about the magnetic dipole axis.

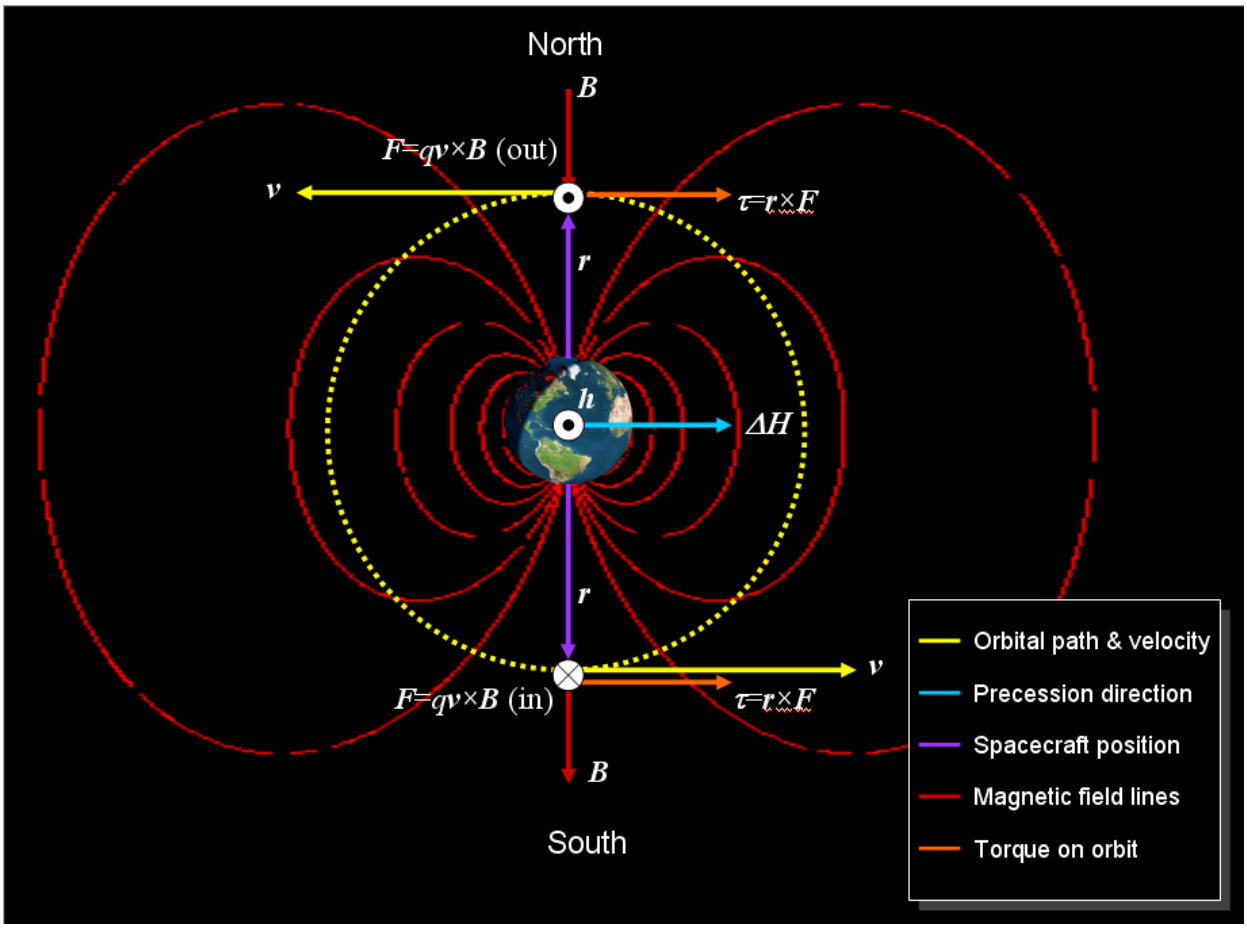

Figure 3. Dynamics of the Geosynchronous Polar Orbit (Altitude Not to Scale)

A near-polar satellite with constant potential precesses around the earth in a way that enables it to cover the same point on the ground each orbit. The orbital plane precesses at 360 deg/day. Thus, it is a geosynchronous (though not geostationary) LEO satellite. The implications for earth observations and communications are game-changing and have attracted the interest of Northrop Grumman Space Technologies. Our recent collaboration with them has brought with it plasma-modeling capabilities and some small additional funding. Appendix A of this report is a draft of a paper on this subject we intend to present at the 2006 AIAA GNC Conference.

Sun or Moon Synchronous Missions: q/m *between 0.01 and 0.1 C/kg*

Since J2 is traditionally used to establish a sun-synchronous orbit—one that precesses 360 degrees per year so that the spacecraft is always in the sun—the Lorentz effect can be used the same way. However, only a very special range of orbital elements can be used for traditional sun-synchronous orbits. In contrast, a sun-synchronous LAO can be of virtually any inclination, and semimajor axis, and any eccentricity (although some extreme cases may require prohibitively high charge). The result is a capability for high-power satellites that need no batteries because they would never enter eclipse.

A related orbit is the moon-synchronous one. This orbit would be inclined so that its plane is normal to the earth-moon line, but it would precess at about 36 degrees per day. The result is a spacecraft in low-earth orbit that is always in view of the moon. Such a satellite could serve as a

communications relay for manned activity on the moon, a power relay for a lunar power-generation station that beams energy back to the earth, for lunar geodesy, or for lunar science.

Long-Duration LEO Mission with J2 Cancellation: q/m *between 0.0001 and 0.01 C/kg*

Lengthening the duration of any LEO spacecraft eliminates one of the primary disadvantages of low-altitude orbits. The work done (i.e. the reduction in orbital energy) by atmospheric drag can be canceled on a per-orbit basis by the Lorentz force, at least for elliptical orbits. In fact, the Lorentz force is highest in LEO, where the magnetic flux is densest, the plasma sheath is thinnest, and the spacecraft velocity is highest. While the effect may require more power than an equivalent electric propulsion system, we emphasize that the LAO requires no propellant. Consequently, the space system's lifetime is not limited by the propellant load, and more payload can be incorporated in place of this saved mass.

Some inclination of the orbit above the magnetic equator allows the same precession effect to act like J2 (the gravitational perturbation due to the earth's oblateness). For the right amount of charge, the J2 perturbation can be canceled, or even reversed.

Earth-Moon Infrastructure Missions: q/m *above 50 C/kg*

The Apollo-era free-return trajectory likely saved the Apollo 13 astronauts. It is probable that the Vision for Space Exploration will employ something similar for earth-to-moon transfer of passengers and freight. However, the Keplerian free-return trajectory is a one-day phenomenon. After returning to the earth, the spacecraft cannot re-enter another free-return trajectory without expending propellant. In contrast, an LAO can be made to precess at a rate that would keep a spacecraft in a continuous Earth-moon trajectory. Such a spacecraft would shuttle back and forth without propellant, leading to an indefinite a free-return-and-back behavior.

The indefinite free-return trajectory can be coupled with a circular LAO that uses the Lorentz effect to match its mean motion at the free-return trajectory's altitude. The result would be a LEO spacecraft that would rendezvous with this resupply spacecraft to load or offload freight (but probably not passengers because of the limited duration of the rendezvous). Thus, the Vision for Space Exploration would have at its disposal a means of conveying freight from LEO to the moon without propellant. Doing so would require very high charge on the LEO spacecraft, but the prospect is so compelling that we propose to pursue it in more depth. Figure 4 shows a schematic of a spacecraft that cycles from LEO to the moon several times per month.

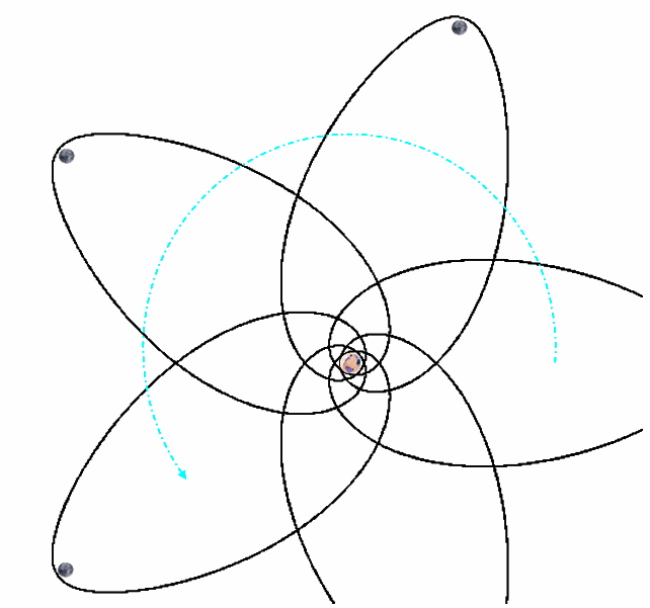

Figure 4. Orbital path of lunar-cycling trajectory. The dashed line shows the direction in which the orbit's line of apsides evolves.

4.2 Key Equations for *q/m* Sizing

This section provides simple equations that can be used to size the all-important *q/m* parameter for the LAO missions described above (and others). Such equations are of great value in systems-engineering efforts to trade technologies against one another and determine a system's technical performance measures.

Table 1. LAO *q/m* Parameter Sizing Equations

Geosynchronous, polar satellite	$\frac{q}{m} = \frac{\omega_E a^3 (1-e^2)^{3/2}}{B_0}$ (elliptical); $\frac{q}{m} = \frac{\omega_E r^3}{B_0}$ (circular)
Geosynchronous satellite in a circular, inclined orbit	$\frac{q}{m} = \frac{\omega_E a^3}{B_0}\left(\omega_E \cos i \frac{a^{3/2}}{\sqrt{\mu}} - 1\right)^{-1}$
Sun-synchronous, moon-synchronous, or other continuously precessing satellite	$\frac{q}{m} = \frac{\omega_{desired} a^3}{B_0}\left(\omega_{desired} \cos i \frac{a^{3/2}}{\sqrt{\mu}} - 1\right)^{-1}$
Arbitrary Geosynchronous satellite	$\frac{q}{m} = \frac{\omega_E a^3 (1-e^2)^{3/2}}{B_0}\left(\omega_E \cos i \frac{a^{3/2}}{\sqrt{\mu}} (1-e^2)^2 \frac{e^2 - [(1-e^2)^{1/2} - 1]^2 \cos 2\omega}{e^2} - 1\right)^{-1}$
Equatorial satellite with precessing line of apsides (ω)	$\frac{q}{m} = \frac{\dot{\omega}_{desired} a^3 (1-e^2)^{3/2}}{2B_0}$

Orbital radius for a desired orbital angular velocity ω	$r = \sqrt[3]{\frac{1}{\omega^2}\left(\mu - \frac{q}{m}(\omega - \omega_E)B_0 R_0^3\right)}$
Angular velocity for a desired rendezvous at a desired orbital radius	$\omega = -\frac{q}{m} B_0 \frac{R_0^3}{r^3} \pm \frac{\sqrt{\left(\frac{q}{m} B_0 R_0^3\right)^2 + 4r^3\left(\mu + \frac{q}{m}\omega_E B_0 R_0^3\right)}}{2r^3}$
Planetary Escape	$\frac{q}{m} = \frac{\dot{a}\mu}{2a^2 B\dot{r}r\omega_e}$ Modulate such that q/m=0 from perigee to apogee

a - orbital semimajor axis
B_0 – magnetic field strength at planet's surface (~3e-5T for Earth)
e – orbital eccentricity
i – orbital inclination
m – total spacecraft mass
μ – planet's gravitational constant
ω – orbital angular velocity or argument of perigee (as specified)
ω_E – planetary spin rate
q – charge
r – orbital radius
R_0 – radius at which B_0 is defined

Concept of Operations

We have identified several operations concepts that take advantage of the peculiarities of an LAO and accommodate what we believe are the means by which charge can be established on the spacecraft. The main features of these operations concepts are the following:

- The plasma environment will bleed off the charge on an LAO-capable spacecraft. The spacecraft will experience discharge less at higher altitudes and at higher latitudes. Inconveniently, the planetary magnetic field is strongest at low altitudes. The most power-efficient LAO may therefore be one that passes near the poles, where plasma density is low and magnetic flux is densest.
    - In a polar mission, the power-efficient approach involves gathering solar power (or charging a capacitor bank via nuclear power) within some latitude range of the equator, and then expending it in a high-energy burst through a plasma contactor or similar charged-beam device near the poles to establish potential at the best possible time. This mission architecture is ideal for the Goesynchronous LEO architecture, the Lunar-synchronous architecture, and possibly for the lunar-rendezvous mission (in which the free-return trajectory has an out-of-plane character).
    - Either the Jupiter-insertion mission or the Earth-escape mission would involve similar operations: charge batteries or capacitors when far from perigee; then, near perigee, expend this stored energy in a burst that maintains a high potential during perigee passage,

where most of the LAO benefit is found. Work is ongoing to come up with an optimal set of timing parameters for such a maneuver.

- Space weather introduces considerable variability into the Lorentz force. The nearly unpredictable variation in plasma density will necessitate closed-loop control of the charge on the spacecraft if precise orbits are required. For grosser effects, such as earth escape or Jupiter capture, using the naturally high potentials due to magnetic storms (e.g. -20kV) will minimize power requirements by taking advantage of the environment.
- An LAO-capable spacecraft must maintain an orbit ephemeris on board and a model (or measurement) of the magnetic field. This requirement flows down to the attitude-control subsystem and the command and data-handling subsystem.
- Orbit raising requires modulated charge. If an appropriate plasma-contactor or ion/electron-beam technology can be found to emit two charged species, both positive and negative charge can be established, cutting the time to escape in half. Otherwise, operations consist simply turning on and off the charge (allowing the plasma to discharge the spacecraft) twice per orbit.

4.3 Enabling Technologies

The Phase I effort focused considerable effort on self-capacitance. There is more work to be done in this area in a follow-on investigation, partly because we continue to discover new solutions that ought to be evaluated in an effort evaluate the viability of the LAO concept for a NASA mission. We also investigated charging/discharging technologies that can work in the variable plasma environment of space. We summarize the results here.

Self-Capacitance

The conceptually simplest architecture is a thin-walled conductive sphere that surrounds the spacecraft. The surface holds charge with a capacitance C given by

$$C = 4\pi\varepsilon_0 R\,, \tag{4}$$

where R is the radius of the sphere and $\varepsilon_0 = 8.8542 \times 10^{-12}$ F/m is the permittivity of free space. The surrounding plasma forms an oppositely charged sheath around such a body, resulting in an increase in capacitance (particularly for a thin sheath):

$$C = 4\pi\varepsilon_0 \frac{R(R+\lambda)}{\lambda}\,, \tag{5}$$

where λ is the thickness of the sheath. In LEO, λ is on the order of a centimeter for low potential and up to several meters for high potentials, offering a possible increase of as much as three orders of magnitude in the capacitance over a sphere in a vacuum if the sphere's radius is on the order of tens of meters. Figure 5 is an artist's rendition of the concept.

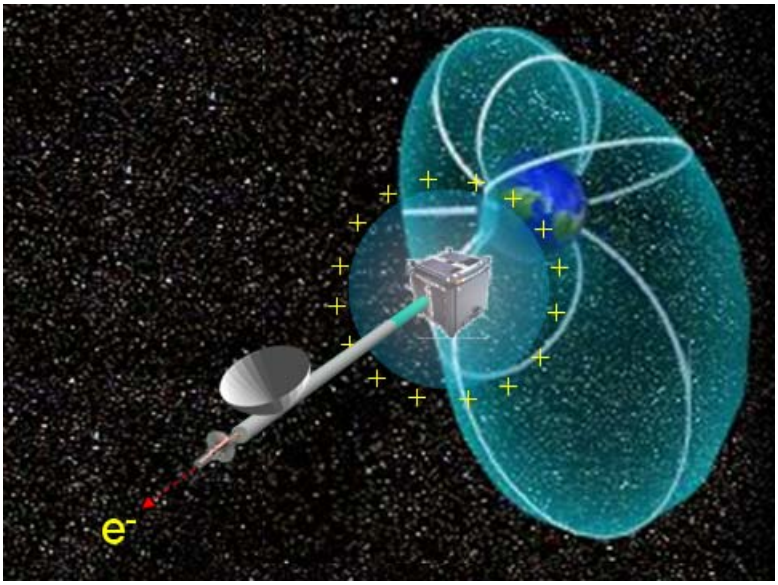

Figure 5. Spherical Capacitor Concept

A far more lightweight option is the use of a thin conductive filament of length L, whose theoretical capacitance is

$$C = 4\pi\varepsilon_0 L\,. \tag{6}$$

This result is independent of the thickness of the wire. While micron-thick wire can be used, the limiting configuration is a fiber consisting of carbon nanotubes. With a capacitance per length of perhaps 4×10^{-11} F/m values of *q/m* approaching 3×10^{6} C/kg can be achieved for a single nanotube. This estimate of capacitance per length for a conducting filament was measured in our laboratory by Mr. Patrick Conrad of Cornell and compares well with theory. Choosing an appropriate length for the spacecraft of interest is a simple matter of scaling from such a value. Micrograms of nanotubes can achieve even the most extreme values of *q/m* proposed to date. In this sense, the carbon nanotubes are very similar to the carbon nanofoam we investigated in the Phase I effort. Some of our Phase I work addressed the preliminaries of constructing a wire-based LAO spacecraft, measuring the capacitance of such a device, and comparing it (successfully) with experiment.

Similar to the thin-wire technology, another approach is the molecular self-capacitor. Certain molecules include non-equilibrium charge. DNA is an example[13]: the unbalanced charge in the base pairs of a human's DNA would represent hundreds of Coulombs if the ionized molecules surrounding the DNA did not cancel the net charge. Figure 6 suggests the process by which this charge shielding operates. Using proteins or polymers that chemically bond the electrons in place increases their possible capacitance beyond the limits of conductors, where the finite work function of the material can ultimately lead to discharge via Coulomb repulsion from the surface. Pulling out these ions, via electrophoresis or other processes, allows the DNA to act as the LAO spacecraft's charge-storage system.

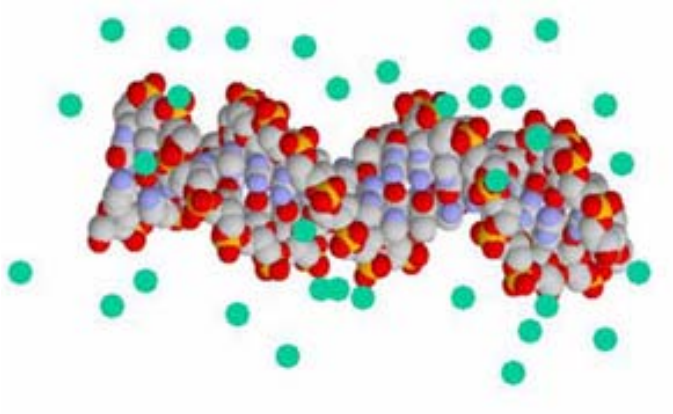

Image courtesy of Dr. Lois Pollack

Figure 6. Positively charged or counter-ions, shown as green spheres, neutralize a large fraction of DNA's negative charge. Electrostatic interactions are used to control DNAs conformation and interaction with other macromolecules.

The inherently charged molecule is surrounded by an electrolytic fluid, which allows charge to travel from the surrounding plasma to the DNA. When biased charge is needed, an electrophoretic process extracts charged particles (ions) and expels them from the surface using an ion beam or an alternative means of emitting charge from the spacecraft. Approximately 30% of these ions can be extracted in such a fashion. Some of the DNA molecules will break under the Coulomb stress that results from their biased charge, but the charges ought to remain embedded in the molecules because this attraction is far greater than the Coulomb forces that can mechanically strain the molecules. Figure 7 illustrates the concept.

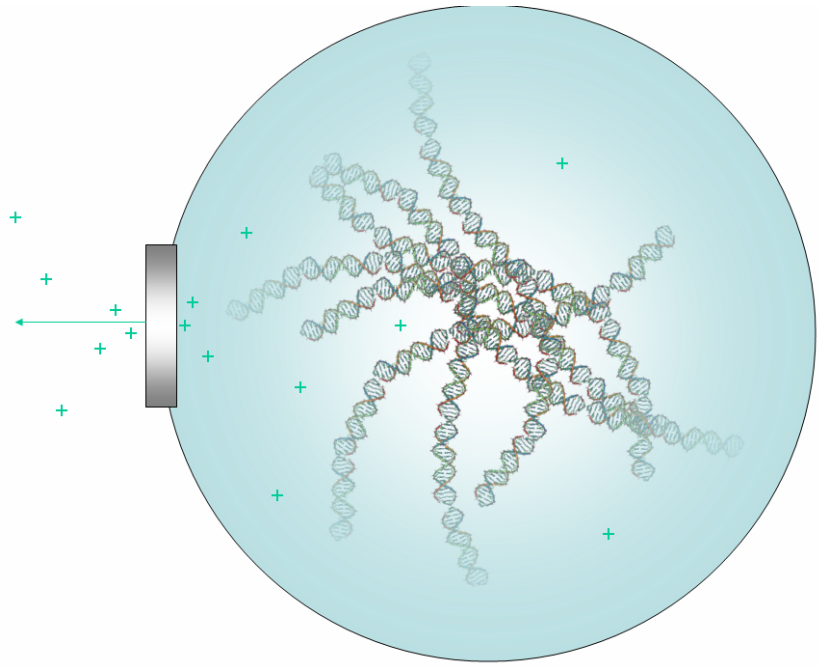

Figure 7. Molecular Capacitor Concept: DNA or other charged molecules are bonded to a central core and suspended in a fluid, from which charge is extracted, leaving an imbalance of charge chemically bonded within the molecules.

Carbon Nanofoam

Carbon nanofoam (or carbon aerogel) is a newly discovered allotrope of pure carbon. It is a semiconductor whose structure consists of a molecular tangle of carbon atoms, arranged such that its effective surface area is about 400 m^2/g. Along with this large surface area comes very high capacitance, about 30F/g. At this capacitance, a 1 kg sample at 1V ought to hold 30,000C, so long as the material itself does not fail under the stored electrical pressure. For the LAO concept, that charge represents q/m=30,000 C/kg. Even the most ambitious applications of an LAO require only tens of C/kg. For example, the geosynchronous LEO orbit requires about 2.8 C/kg. Figure 1 shows several samples that we analyzed during the Phase I study.

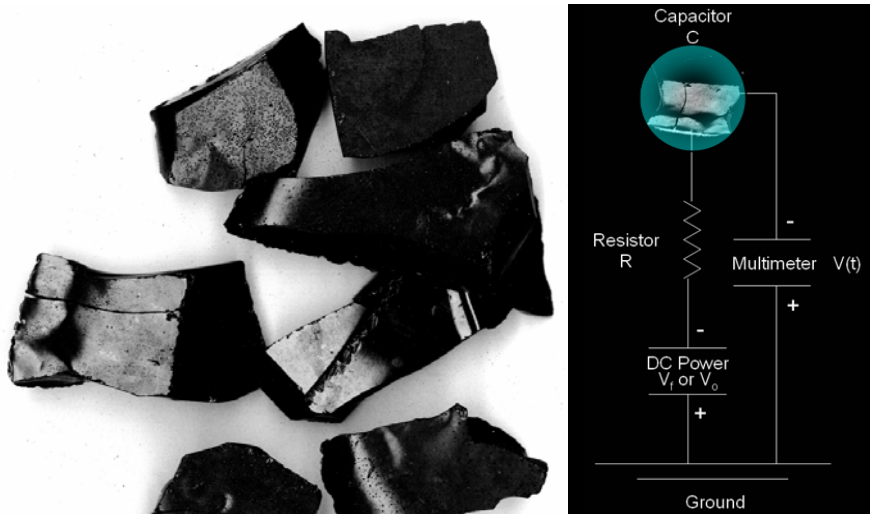

Figure 8. Carbon Nanofoam Samples and Schematic of Test Setup

Figure 9 through Figure 12 are scanning-electron microscope (SEM) photographs of carbon nanofoam samples we procured. The photographs were taken at Cornell's Center for Nanofabrication (CNF) by Bernardo Cordovez of the Erickson Laboratory. The objective in imaging it is to verify the structure at the nanometer level. These images confirm that the structure is quite convoluted, at least down to the 2 nm level. Of particular relevance to the LAO project is the fact that the electron beam used in this experiment charged up the material, thereby deflecting the beam and resulting in blurry images. This behavior demonstrates precisely what we hope for in this material, although the SEM photographs offer no way of evaluating the amount of charge stored during the imaging process.

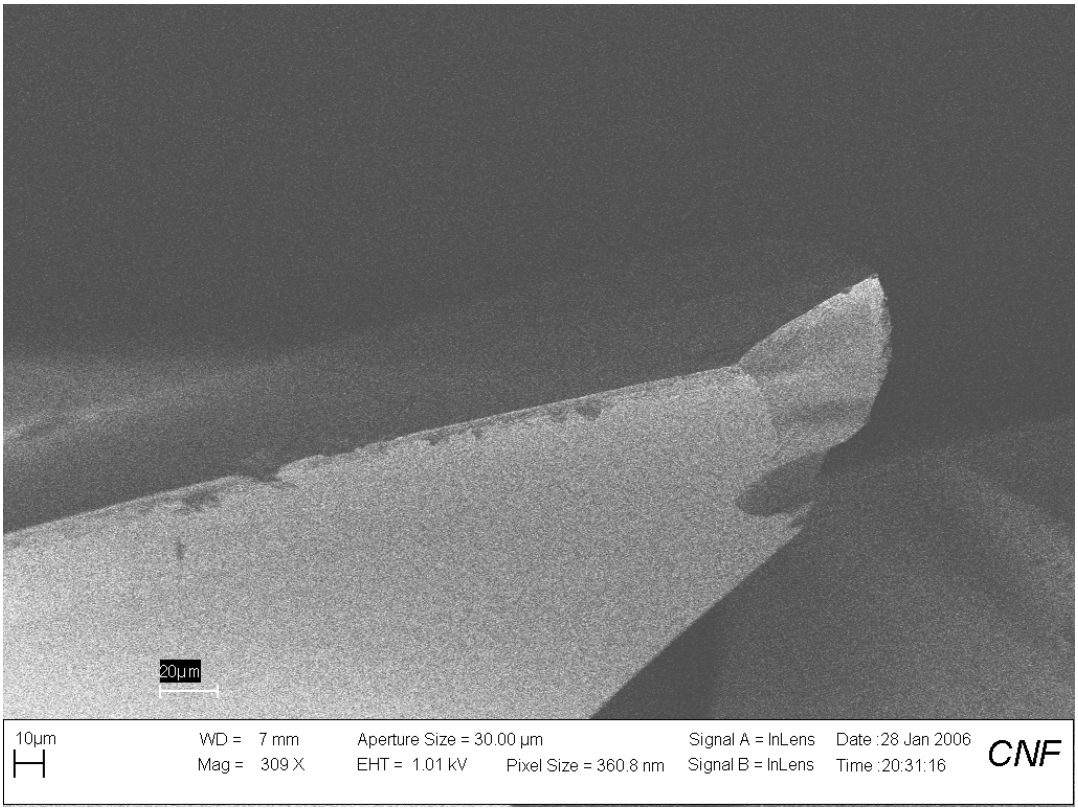

Figure 9. 360.8 nm Resolution SEM Photograph of Carbon Nanofoam.

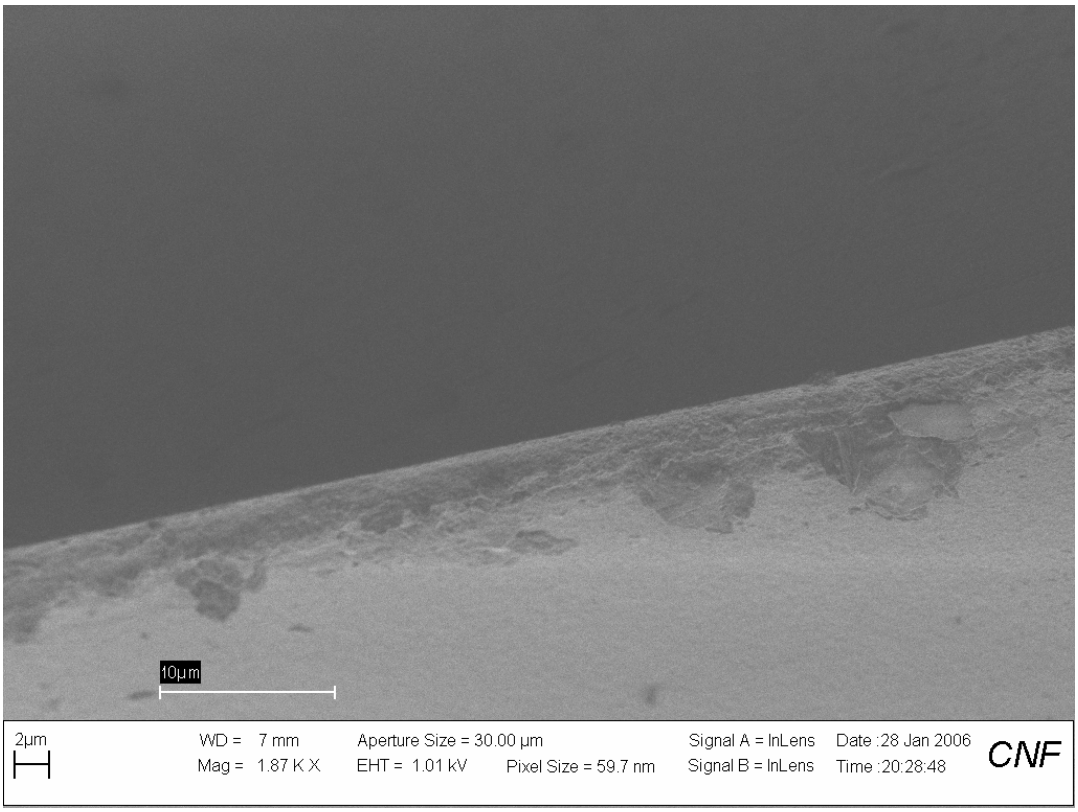

Figure 10. 59.7 nm Resolution SEM Photograph of Carbon Nanofoam.

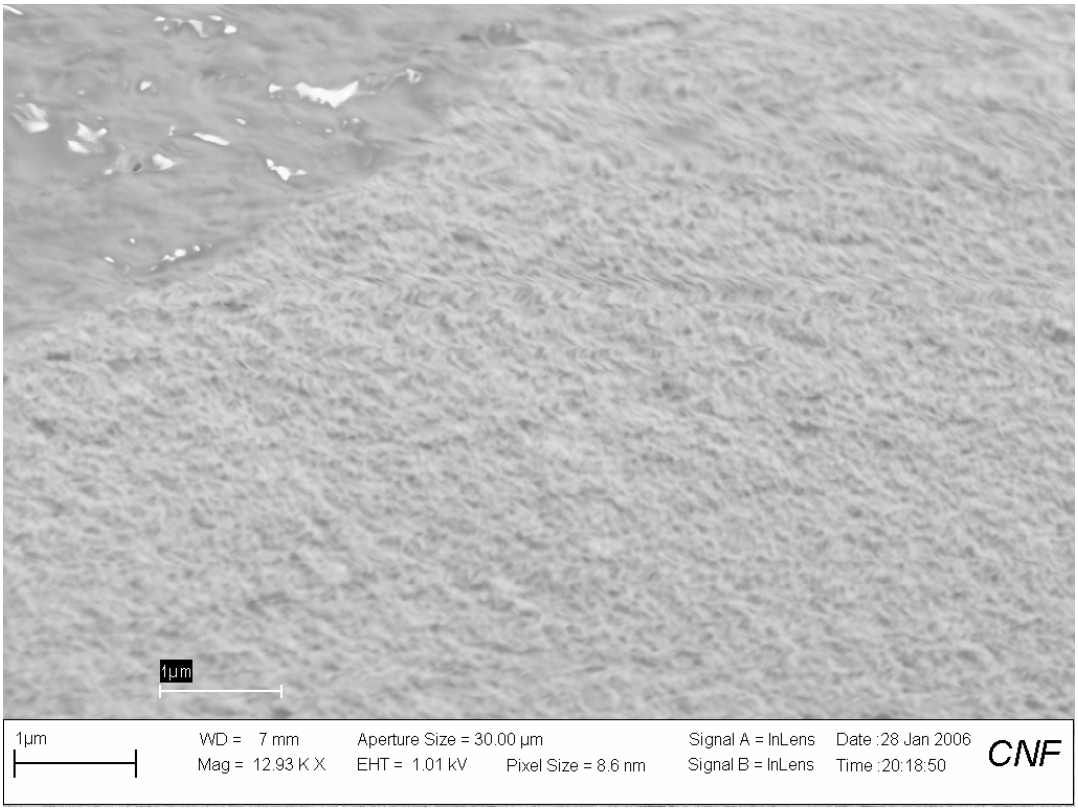

Figure 11. 8.6 nm Resolution SEM Photograph of Carbon Nanofoam.

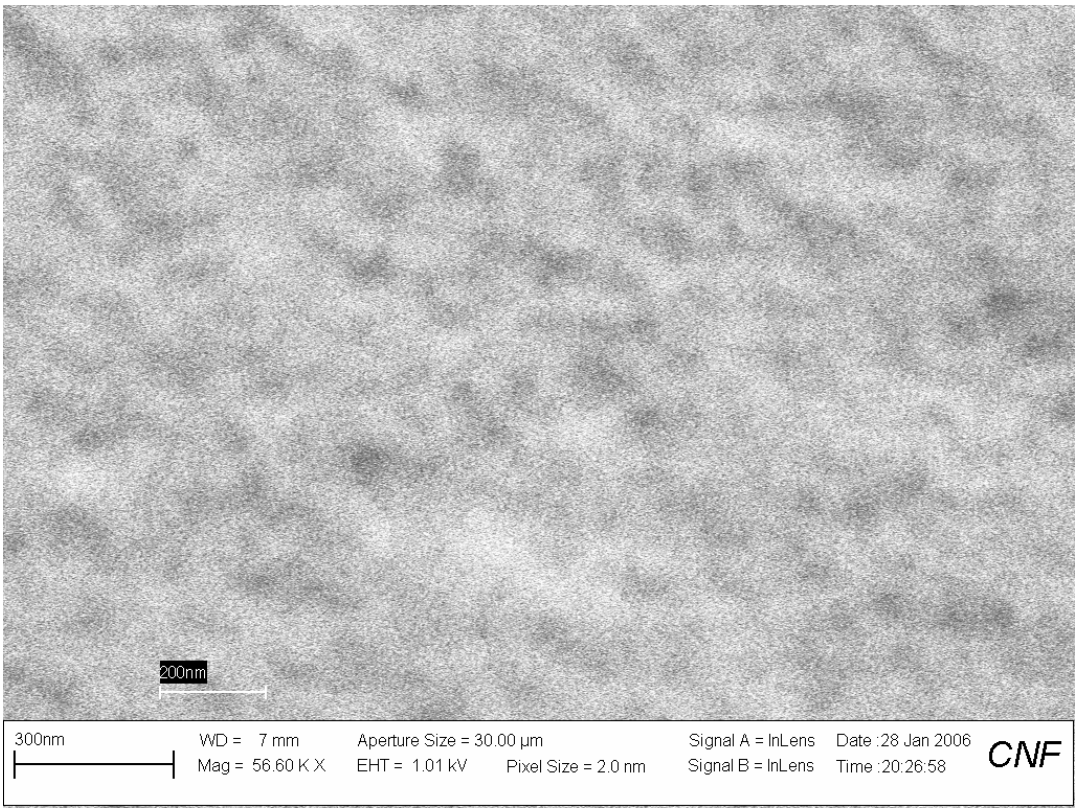

Figure 12. 2.0 nm Resolution SEM Photograph of Carbon Nanofoam.

This extraordinary material was so promising that we diverted some of our effort to testing it in the hope of demonstrating the promised properties. These tests included attempts to establish a charge within the material and to measure its tensile strength. The test setup consisted of a constant-current power supply and a 5g sample of nanofoam in series with a known resistance in a configuration that allowed the power supply to drive the voltage of the nanofoam to a steady state. The experiment was unable to show self-capacitance at the level required by an LAO. Therefore, we have not been able to identify this material as the solution for capacitance. It may be the case that using this material with an electrolyte, similar to the molecular-capacitor concept, will prove fruitful.

Power

As important as holding the charge is the problem of fighting the plasma, which continually tries to discharge the spacecraft (or at least bring it to a floating potential). Power is required for this purpose. Naturally, one would optimize the power usage by storing energy (e.g. from solar power, in batteries) when no charge is required, and then expending it to maintain the charge when the Lorentz interaction benefits the mission. The current to the spacecraft depends on the cross-sectional area of the charged structure plus its sheath, and the number (and type) of charged particles this area encounters as this area sweeps out a tunnel through the plasma. That total becomes a current. The power required to maintain charge in the presence of that current is simply the product of the incident current and the spacecraft surface potential.

The current depends on electron and ion number density. In equatorial LEO, the ion current is 6e-4 A/m^2. The electron current is 3.5e-6 A/m^2. The sheath's contribution to this area grows with voltage. For tiny potentials in LEO it is centimeters in scale and is negligible. For thousands to millions of volts, the sheath thickness in LEO is 10-50 m. A further complication is that in regimes where these densities change, such as a polar orbit, the power depends on orbital position. As an extreme example of size, we have calculated that at a 100 m, 50 kV sphere in LEO collects about 4.6A of current, for a total power of 230 kW. The high power required by a sphere inspires the ligher, smaller-cross-section solutions described above.

Generally the LAO spacecraft can require hundreds to hundreds of thousands of Watts. This range depends entirely on the size of the capacitor and sheath (which derives from the payload weight) and the spacecraft potential. Some of the architectures we propose to evaluate in the future are capable of maintaining charge at low potential because they are so highly capacitive. The molecular capacitor and the carbon nanotubes are examples, where enough charge may be available even at the plasma floating potential to achieve the propulsion requirements of an LAO mission.

Counteracting discharge into the plasma with an electron beam or an ion beam is the low-risk approach, but it comes at a heavy price: specific power (the power per weight). To achieve a high *q/m* a far more successful approach may be to use pyroelectric crystals. These materials emit electrons and ions at high energies (~10^5 eV) when their temperature changes. Spacecraft beam-charging experiments have shown that spacecraft potential approaches the beam energy for sufficient current, and so we expect that this technique promises hundreds of kV of potential at the spacecraft surface.

Accelerating charge away from the spacecraft using this highly efficient approach is a topic we intend to explore with James Brownridge at SUNY Binghamton, the researcher who first brought the prospect of self-focused ion beams from these materials to the attention of the scientific community[14]. He has shown that certain pyroelectric crystals (e.g. $LiNbO_3$ and $LiTaO_3$) produce

electron and positive ion beams during heating and cooling in dilute gases. These beams are self-focused and exhibit beam energies as high as 113 keV. This lightweight but highly effective means of producing high-energy beams may allow an LAO-capable spacecraft to operate with a much higher charge-to-mass ratio. Its TRL is probably 2.

There are other promising approaches of low TRL. One is to take advantage of the photoelectric effect (or Hertz effect) by using a large amount of material from which sunlight drives off electrons. A similar approach might be taken with material that is driven negative in eclipse due to electron impingement. In both cases, directing the perigee of the LAO so that the natural charging occurs at the time when one wishes to take advantage of the Lorentz force may obviate the need for an active charging mechanism.

An even more promising avenue is the use of alpha-emitting radioisotopes. These materials emit charge in the form of alpha particles (helium nuclei, which carry two fundamental positive charges) at high energies, beyond 5 MeV. Small quantities of commercially available Polonium 210, which has been used for static-electricity control, can offer significant power-to-weight advantages over any other power technology identified to date. Because we use this isotope for its alpha decay explicitly, rather than to run a radioisotope thermoelectric generator, its power-to-weight is very high. 1 kg of this material, spread thinly on the outside of the spacecraft, can generate 90kW of alpha particles even after one year's decay, with a current of 0.034 A and a spacecraft voltage of over 5 MV. We re-emphasize that this use of nuclear material is not as a traditional nuclear fuel for thermodynamic energy extraction, which typically offers only a few W/kg. Instead, the high-energy alpha particles are used to counteract plasma discharging and maintain a potential of 5 MV at the spacecraft's surface.

Plasma Interactions

A plasma sheath forms around a charged body. The sheath is of opposite polarity and equal charge. It shields electric fields, virtually eliminating the possibility of Coulomb interactions beyond distances of the Debye length: 1 cm - 10 m in Earth orbit. The plasma surrounding an LAO spacecraft does not travel with the spacecraft. Like the changing pressure of air flowing over a wing, the plasma's charge distribution changes in the neighborhood of the spacecraft. However, when the spacecraft has passed, its charge distribution returns to that of the ambient plasma. Since the plasma does not travel at spacecraft velocity, it feels no Lorentz force. That conclusion is important because if the plasma sheath were to experience the Lorentz force, its opposite polarity would cancel the body's Lorentz force.

The plasma also has the beneficial effect of reducing or even eliminating the mechanical pressure exerted by the charge on the surface of the sphere, which might otherwise cause it to fail, or pop. Our Phase I study showed that while simple, the sphere architecture cannot realistically maintain charge-to-mass (q/m) beyond a fraction of a Coulomb per kilogram.

This shielding can increase capacitance, and so it is not entirely unwelcome. As explained, it also tends to balance electrostatic pressure s that the material's tensile strength does not limit the charge that can be stored. Instead the limits arise from coulomb repulsion from the surface, especially when the surface is rough, which can occur below 1MV. The DNA capacitor described above is not subject to this limit because the charge is inherent in the molecules.

Plasma shielding introduces a concern about telemetry and command for the spacecraft. One solution is to use laser communications, which require only an optical path. Alternatively, an antenna may protrudes through the Faraday cage (introducing some ESD issues). A concept is

shown in Figure 13. Figure 14 shows a conceptual plasma sheath and a numerical example computed by NASA's Charging Analyzer Program (NASCAP). NASCAP computes an eccentric sheath, which is caused by the spacecraft traveling at orbital velocity, compressing the sheath forward of the spacecraft and elongating it aft.

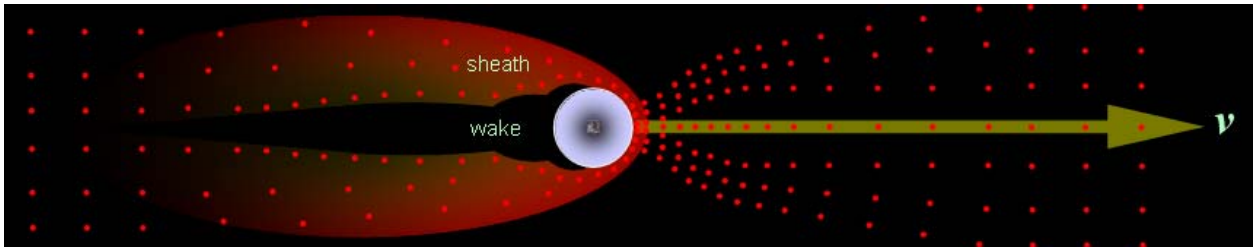

Figure 13. LAO spacecraft traveling at high velocity, leaving a wake in the plasma.

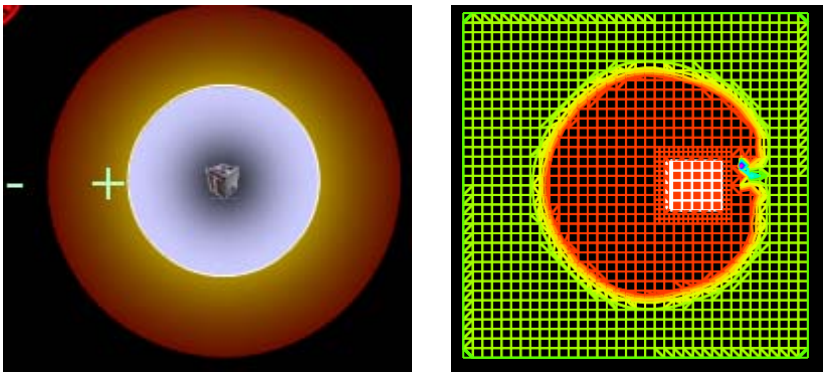

Figure 14. Conceptual Plasma Sheath (left) and NASCAP Analysis at 1 kV inLEO (right).

4.4 Performance Comparisons

Electrodynamic tethers and solar sails certainly have their place. Tethers are convenient for de-orbiting spacecraft in a passive way (i.e. without applied power). Solar sails work just as well, if not better, outside the geomagnetic field as they do near the earth. However, both suffer from the problem that the very large structures involved can deform under the action of the forces on them, reducing their performance. In the case of a tether, it appears that only gravity-gradient balance or spinning will help align a tether stiffly enough for it can raise an equatorial orbit in a mass-efficient way without buckling, tangling, or becoming redirected into a useless orientation. Solar sails are virtually impossible to reorient in an agile fashion. Our goal is to develop the LAO concept to the point where it is highly compact but offers the same propellantless benefits. The result will be an agile propellantless spacecraft. Even if the LAO spacecraft includes a long wire for capacitance, this wire will result in the same effect regardless of its direction. This significant advantage argues for the continued investigation of the LAO concept and suggests that it may prove more readily adaptable to existing mission architectures than are tethers.

Here we summarize two example missions in an effort to demonstrate the value of an LAO: the geosynchronous LEO mission and the Jupiter capture mission. More examples are offered in the Phase I report.

Synchronous LEO Performance Example

In order for a tether to achieve a polar, synchronous orbit of the type described in Section 4.1, the tether current (and therefore the tether) must be in the along-track direction of the satellite. By contrast, the LAO spacecraft's "current" consists of its own motion along its path, guaranteeing a correct alignment of the electrodynamic force. Although the flexible-body dynamics of a tether along the velocity direction of the spacecraft are non-trivial, here only the electrodynamic considerations will be addressed. This simplification represents a best case for the tether.

With an along-track electrodynamic tether, the Lorentz force experienced by a satellite is equivalent to the Lorentz force on an LAO satellite. These two terms can be equated as

$$q\boldsymbol{v} \times \boldsymbol{B} = L\boldsymbol{J} \times \boldsymbol{B} \tag{7}$$

where the left side of the equation represents an LAO satellite, and the right a tether. Solving for the length of tether required to approximate an LAO satellite of charge q and mass m gives

$$L = \frac{qv}{J - \frac{q}{m} v\lambda} \tag{8}$$

where v is the orbital velocity of the LAO satellite and λ is the mass per unit length of the tether. As the tether length cannot be negative, the denominator of this equation must be positive, giving rise to a minimum required tether current of

$$J > \frac{q}{m} v\lambda \tag{9}$$

For a polar GT-1 LAO satellite at an altitude of 400km and q/m=2.83 C/kg, and using the aluminum tether described by Forward et al.[15], a commonly cited tether length of 20 km, and a spacecraft base mass of 10 kg demands a 55 A current. A thin aluminum wire simply cannot withstand such a high current. Thicker tethers add mass to the point of diminishing returns, even without considering the mass of the tether's power system. We conclude that the LAO is the only way to realize such a mission.

Generally speaking, tethers suffer from an inability to remain stiffly aligned with their desired direction. Using the gravity-gradient effect to establish a kind of torque equilibrium addresses this issue for tethers that are directed radially from the center of the planet. In the GTO case and in many other cases of interest, tethers cannot benefit from gravity-gradient stabilization. By contrast, even if an LAO uses a thin fiber to hold the charge, this fiber can be oriented anywhere without affecting the Lorentz force, and regardless of the gravity-gradient torque.

Jupiter Capture Performance Example

Jupiter has two key features that identify it as an ideal target candidate for Lorentz maneuvers. The first is that Jupiter has the highest rotation rate of the solar planets, 2.4 times that of Earth. The second is its powerful magnetic field, both in terms of range and energy. Jupiter's magnetosphere is the largest planetary structure in the solar system, with a tail that extends beyond Saturn. This field also contains a great deal of energy, roughly 20,000 times that of Earth's magnetosphere. These two characteristics make the Lorentz force most pronounced at Jupiter, thus making it an ideal environment for Lorentz propulsion. We compare the Galileo insertion[16] to an LAO mission requiring similar ΔV.

A series of interplanetary flybys provided the initial conditions for an extensive series of Jovian orbits and moon flybys that lasted eight years. Though successful, these maneuvers have clear disadvantages. Reliance on flybys introduces a great deal of complexity in mission planning and restrictions on launch windows. Thruster use adds to the spacecraft total mass--in this case, 371 kg of propellant. Eliminating this significant mass represents an opportunity for increased payload mass or decreased launch cost.

Our approach is for the spacecraft to insert into Jupiter orbit, a capture maneuver we defined via a final energy that meets the mean tour energy (found by averaging the semi-major axes of the first ten Galileo tour orbits.) The LAO spacecraft can capture with q/m= between 0.113 and 0.2 C/kg, requiring no more than 284 days and as few as 25 days to spiral inward to an orbit comparable to Galileo's.

5. Conclusions

The phase 1 study accomplished its goals of identifying directions for technological development necessary if the LAO concept is to become a viable space system. It also established that the LAO concept's prospective contribution to future NASA efforts is the liberation of spacecraft missions from the classical Keplerian orbit. All the remarkable applications we have identified to date represent time varying classical orbital elements but relative equilibria of this subtle Hamiltonian system. Figure 15 shows these prospects in terms of the driving design parameter of the LAO system, q/m. The new applications of existing technologies represent our preliminary assessment of straightforward mechanical solutions for storing charge and maintaining it. The stretch technologies involve the more futuristic concepts, such as the DNA-driven spacecraft.

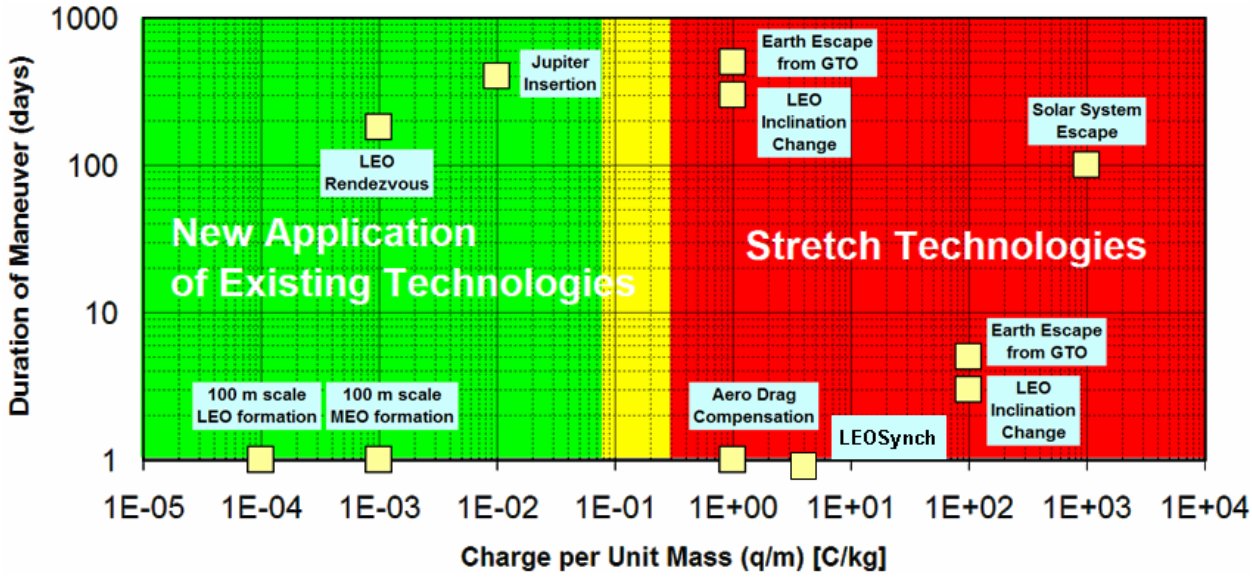

Figure 15. Present and Technology-Stretch Capabilities for the LAO

The technology-development issues consist of the three overlapping areas described in this report: capacitance, charge maintenance, and plasma interactions. **Table 2** summarizes the capacitor concepts and estimates their performance and TRL.

Table 2. Capacitor Performance Summary

Capacitor Solution	**Maximum *q/m***	**Power Required**	**TRL**
Conductive Sphere	0.02	1 kW-1MW	5
Macroscopic conductive filaments	0.04	1 kW-1MW	4
Nanotube filaments	No limit identified (very high)	0W-1kW	1
Molecular capacitor (DNA)	No limit identified (very high)	0W-1kW	1

These concepts' required power can be misleading, suggesting that no near-term power system can sustain an LAO. However, we have identified options with high specific power for this particular application. These options are summarized in Table 3.

Table 3. Charging Power Sources (Charge Maintenance)

Charging Technology	**Maximum *W/kg***	**TRL**
Solar Photovoltaic	300[17]	10
RTG	20[17]	8
Nuclear Reactor	40[17]	1
Pyroelectric Crystals (113 kV potential)	unknown	1
Bare Polonium 210 (5.3 MV potential)	560,000 at t=0 90,000 at t=1 year	1

An important conclusion is that there is a trade-off between capacitor TRL and power subsystem TRL. The high-capacitance devices require little power, and may even operate adequately on the plasma's floating potential. The power risk is therefore minimal. Conversely, the low-risk, low-capacitance approaches demand high power density to maintain q/m. Our hope is that future work will confirm which end of this trade space offers the most promise. Our Phase I work suggests that high-capacitance solutions are where future efforts should be focused.

The plasma-interaction issues are summarized above. Modeling them poses particular challenges. Future work will involve evaluating existing codes, such as NASCAP, for their accuracy in predicting power and charging interactions to help evaluate capacitance and power technologies. If their fidelity is as promised, existing codes may provide sufficient predictive capability for us to evaluate an LAO mission architecture in detail, at a resolution better than the order-of-magnitude precision we have been able to achieve in this study.

6. References

[1] Burns, J. A. and Schaffer, L., "Orbital Evolution of Circumplanetary Dust by Resonant Charge Variations," *Nature,* Vol. 337, No. 6205, pp. 340-343, January 26, 1989.

[2] Schaffer, L. and Burns, J. A., "The Dynamics of Weakly Charged Dust: Motion through Jupiter's Gravitational and Magnetic Fields," *Journal of Geophysical Research*, Vol. 92, No. A3, pp. 2264-2280, March 1, 1987.

[3] Cui, Chunshi, and Goree, J., "Fluctuations of the Charge on a Dust Grain in a Plasma," *IEEE Transactions on Plasma Science*, Vol. 22, No. 2, April 1994.

[4] Tribble, Alan C., *The Space Environment: Implications for Spacecraft Design*, Princeton University Press, 2003.

[5] James, B. F., Norton, O. W., and Alexander, M. B., "The Natural Space Environment: Effects on Spacecraft," NASA Reference Publication 1350, November 1994.

[6] Garrewtt, H. B. and Whittlesey, A. C., "Spacecraft Charging, An Update," *IEEE Transactions on Plasma Science,* Vol. 28, No. 6, December 2000, pp. 2017-2028.

[7] Rustan, P., Garrett, H., and Schor, M. J., "High Voltages in Space: Innovation in Space Insulation," *IEEE Transactions on Electrical Insulation* Vol. 28, No. 5, October 1993.

[8] Mandell, M. J., Jongeward, G. A., Cooke, D. L., and Raitt, W. J., "SPEAR 3 Flight Analysis: Grounding by Neutral Gas Release, and Magnetic Field Effects on Current Distribution," *Journal of Geophysical Research*, Vol. 103, No. A1, pp 439-445, January 1, 1998.

[9] Friedrich, M., and Torkar, K. M., "Plasma Observations of the Active Mother-Daughter Payload MAIMIK in the Lower Thermosphere," *Planetary and Space Sciences* Vol. 39, No. 3, pp. 453-467, 1991.

[10] Lai, S. T., An Overview of Electron and Ion Beam Effects in Charging and Discharging of Spacecraft," *IEEE Transactions on Nuclear Science*, Vol. 36, No. 6, December 1989.

[11] Lai, S. T., "On Supercharging; Electrostatic Aspects," *Journal of Geophysical Research*, Vol. 107, No. A4, 2002.

[12] Bilen, S. G., Gilchrist, B. E., Bonifazi, C., and Melchioni, E., "Transient Response of an Electropdynamic Tether System in the Ionosphere: TSS-1 First Results," *Radio Science*, Vol. 30, No. 5, pp. 1519-1535 Sept.-Oct. 1995.

[13] R. Das, T. T. Mills, L. W. Kwok, G. S. Maskel, I.S. Millett, D. Doniach, K. D. Finkelstein, D. Herschlag and L. Pollack, "Counterion distribution around DNA probed by x-ray scattering" *Phys. Rev. Lett.,* 90, 188103, 2003.

[14] J. D. Brownridge, S. M. Shafroth, D. W. Trott, B. R. Stoner and W. M. Hook, "Observation of Multiple Nearly Monoenergetic Electrons Production by Heating Pyroelectric Crystals in Ambient Gas," *Appl. Phys. Lett*. 78, 1158, 2001.

[15] R.L. Forward, R.P. Hoyt, C. Uphoff, "The Terminator Tether™: A Low-Mass System for End-of-Life Deorbit of LEO Spacecraft," Tether Technical Interchange Mtg, Huntsville, AL Sept 10 1997.

[16] Solar System Media Relations, Jet Propulsion Laboratories. http://www2.jpl.nasa.gov/galileo/4800 Oak Grove Drive, Pasadena, CA 91109

[17] Wertz, JR and WJ Larson, eds. *Space Mission Analysis and Design*. 3rd Ed. Microcosm Press, 1999.

Appendix A

Synchronous Orbits and Disturbance Rejection Using the Geomagnetic Lorentz Force

Brett Streetman and Mason A. Peck

To be presented at the 2006 AIAA GNC Conference

Synchronous Orbits and Disturbance Rejection Using the Geomagnetic Lorentz Force

Brett Streetman* and Mason A. Peck †

Cornell University, Ithaca, New York 14853

New forms of Earth synchronous orbits are found using Lorentz Augmented Orbits (LAO). The LAO concept is a propellantless electromagnetic propulsion system without a tether that uses the interaction between an electrostatically charged satellite and the Earth's magnetic field to provide a useful thrust. The equations of motion for such a spacecraft are derived using a non-tilted dipole magnetic field. For a polar orbiting craft, a method of arbitrary control of the angle of right ascension is found, which allows for single orbit repeat groundtrack LEO satellites. Analytical expressions for changes in orbital elements due to Lorentz forces are tested by numerical simulation for the polar and equatorial orbiting cases. In the equatorial case, arbitrary control of the longitude of perigee is found. Perigee control also allows for the creation of an Earth synchronous type of orbit.

I. Introduction

In their earliest forms, man-made satellites were a technology looking for an application. Now, almost 50 years later, satellites have changed the way we live, work, and learn. Many of the space assets now considered indispensable make use of repeat groundtrack orbits. A repeat groundtrack orbit is any orbit whose sub-satellite point traces out a repeatable pattern in some integer numbers of orbits. Traditionally, these orbits are accomplished by adjusting the period of a satellite such that it completes an integer number of orbit in exactly an integer number of sidereal Earth days.

Geostationary and Geosynchronous orbits are perhaps the most readily identified and used repeat groundtrack orbits. These orbits have a mean motion equal to the spin rate of the Earth. We shall refer to orbits that repeat their groundtrack every orbit as GT-1 orbits. Thus all GEO orbits are in the GT-1 class. We define a general notation of a GT-x class orbit repeats its groundtrace every x orbits. While GEO may be the most obvious repeat track orbit, many others systems use these ideas as well. Satellites in the GPS constellation are in 12-hour sidereal orbits, and can thus be considered GT-2 satellites. Many LEO, full-Earth coverage imaging satellites also use repeat trace orbits. Landsat 7 covers the full Earth every 233 orbits making it a GT-233 satellite. Every 16 days, the satellite completes exactly 233 orbits.

Single orbit repeat track paths (GT-1 orbits) have proven quite useful in the development of space technologies. Dedicated weather satellites, constant contact communications, television and radio broadcasts are just a few of the numerous uses for GT-1 orbits. However GT-1 systems are currently limited to GEO orbits. The altitude of these satellites, some 36000km above the Earth's surface, creates problems in communications losses and lower resolution data collection. An ideal case would be a GT-1 orbit at a low Earth altitude. We propose a method of obtaining a low Earth, polar GT-1 orbit in the form of a new propellantless propulsion system called Lorentz Augmented Orbits.

The Lorentz force experienced by a particle of charge q in Coulombs moving through a magnetic field $\vec{B}$ is given by

$$\vec{F}_L = q v_r \times \vec{B} \tag{1}$$

where v_r is the particle velocity with respect to the magnetic field. This force, named after Dutch physicist and Nobel Prize winner Hendrik Lorentz, is used to provided meaningful propulsive actuation in a Lorentz

*Graduate Research Assistant, Department of Mechanical and Aerospace Engineering, 245 Upson Hall, AIAA Student Member.

†, Department of Mechanical and Aerospace Engineering,

Augmented Orbit (LAO). An LAO system makes use of the interaction between the Earth's geomagnetic field and an electrostatic charge built up on a satellite. Thus, LAO is a form of electromagnetic propulsion that does not require a tether. In general the system works as follows: a spacecraft uses electrical power to build up a net static charge on its body and this net charge causes an interaction between the geomagnetic field and the craft in the form of the Lorentz force. The magnitude and direction of the force are defined by the size of the charge on the satellite, the velocity of the craft with respect to the magnetic field, the strength of the magnetic field. Note that in an inertial frame the geomagnetic field rotates with the Earth and has a velocity of its own; the velocity that defines the Lorentz force is the difference between the absolute spacecraft velocity and the velocity of the magnetic field at that point. The power system of the satellite can then actuate the net charge to control the propulsive force.

The LAO system allows for propellant-free propulsion. The energy stored in Earth's rotating magnetic field is used to provide forces on the craft. The size of the force is only limited by charge-holding capacity and power constraints of the satellite. However, the direction of thrust is fixed with respect to the velocity direction of the spacecraft and the direction of the magnetic field. This direction limitation is not so restrictive as to render the system useless, though. With smart planning and intelligent orbit design, many extremely useful applications be actuated using an LAO system. Described below are adding methods orbit raising and lowering, changing orbit angular momentum (both magnitude and direction), and arbitrary right ascension control for low Earth polar orbit. Arbitrary right ascension angle control allows for many exciting possibilities, such as GT-1 and sun-synchronous orbits at any altitude.

II. Related Work and Concept Overview

The Lorentz Augmented Orbit system builds on previous research in many fields. Some of this work is presented here, along with some of the issues and complexities inherent in the system and a possible system architecture for implementation of an LAO.

A. Related Work

The phenomenon of Lorentz force disturbed orbits has been observed in natural systems[1,2] Schaffer and Burns have developed the dynamics of dust particles charged by the plasma environment around Jupiter. They have shown that the motions of these small charged grains can be greatly affected by Lorentz mechanics. This mechanism can be used to explain sparse, latitudinally-thick rings found around Jupiter's main rings. While the dynamics of these particle is mainly well understood, we seek to find applications for controlled-charge spacecraft in a variety of orbits.

Just as dust grains naturally achieve some nonzero charge around Jupiter, a satellite orbiting in a plasma environment will attain a static charge. Many Earth orbiting missions have measured this effect, such a the SCATHA mission.[3] Garrett and Whittelsey[4] present an overview of the natural charging that occurs in the Earth environment. Spacecraft around Earth tend to naturally hold a negative charge, and this charging up occurs with a very fast time constant.[5]

If we wish to control the charge on the spacecraft, the craft must exchange charge with the plasma environment in some way. One possible solution involves the uses of ion or electron beams. The use of these beams has been extensively studied in conjunction both missile defense and ionospheric conditions investigations. AN overview of beam effects on satellites can be found in Lai.[6] In fact, Hough[7] describes the trajectory perturbations on a ballistic missile due to Lorentz force. However, this work is the only study of the effect of the Lorentz force on a spacecraft's orbit that has been found by the authors. The LAO system for orbital control was first proposed by Peck[8]

Other studies have proposed various ways to use charged spacecraft and magnetic field interactions for many applications. Schaub,[5] et al., and Schaub[9] present the idea of Coulomb spacecraft formations (CSF). In this system, satellites in a formation are electrostatically charged and some measure of formation control is given by the Coulomb forces between the various satellites. The CSF system faces many of the same system architecture challenges as the LAO system. However, due to plasma restrictions, a CSF is impractical in LEO, while an LAO is more effective in LEO where the magnetic field strength is greater.

Another electromagnetic formation system is proposed by Kong,[10] et al. Their Electromagnetic Formation Flight system uses superconducting dipole electromagnets on individual satellites in a formation to actuate formation keeping. Interaction between these magnets and the geomagnetic field was not expressly

considered in their study.

One further application of charged satellites in a magnetic field is given by Tikhonov.[11] He proposes the use of nonuniform charging on a satellite to control attitude via the Lorentz force. This idea faces many of the same challenges and dynamics as the LAO systems, but will not be expressly considered here.

B. Issues and Complexities in the LAO System

In an ideal case, the dynamics of an LAO would be relatively benign and simple. In this ideal world, the geomagnetic field would be a simple dipole, the magnetic north pole and the true north pole would be perfectly aligned, and the space environment would be a true vacuum. Of course, none of these things are true. The Earth's magnetic field is a highly complex construction best described by a many term spherical harmonic expansion. The solar wind also causes large spatial and temporal deformations to the field. In addition, magnetic north does not align with true north; magnetic north is about 10° south of the true pole. And because the field rotates with the Earth, the relationship between the two poles is not constant in time.

The Earth's plasma environment is also highly complex. Plasma composition, temperature, and density vary both spatially and temporally in ways that are not well understood. The interactions between a charged satellite and the plasma is also difficult to model, and is affected by the above quantities. Thus, it is hard to model the charge decay of the satellite in a plasma field.

The scope of this introductory LAO study will not cover most of the complexities listed above. Most cases here will assume a non-tilted dipole geomagnetic field. The implementation of an LAO system will only briefly be discussed, and most of the paper will assume that a required charge on the satellite can be delivered, regardless of plasma environment or power constraints. This paper will focus on the basic orbital dynamics of an LAO, and present applications inspired by these results.

C. Possible System Architecture

The LAO system is relatively open system to implement. Any method that achieves a certain electrostatic charge on the satellite will bring about the same orbital dynamics. The design considerations then involve power, environmental interaction, and operations interference issues. By "operations interference," we mean the effects of having a highly charged bodies present on the other subsystems of the spacecraft. Such effects include communications interference, influences on power generation, and electrostatic discharge between components, among other things.

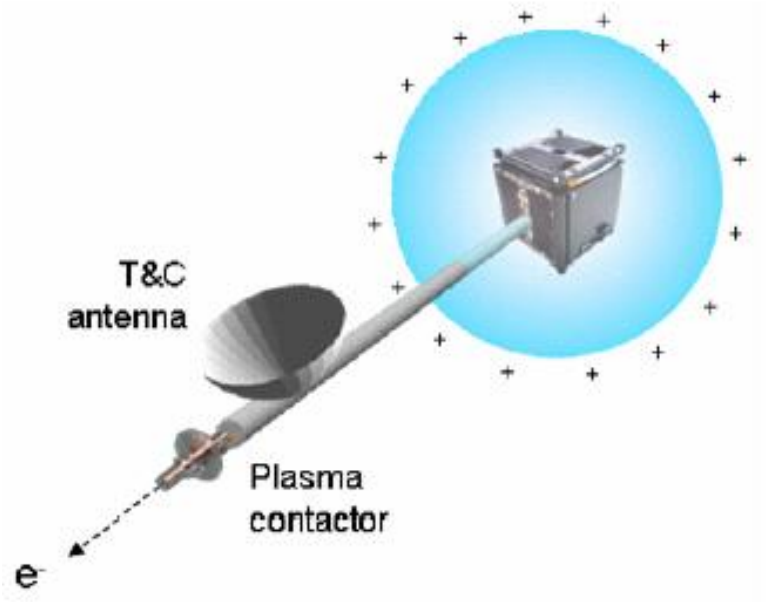

Figure 1. Possible LAO System Architecture

One possible system architecture is shown in Fig. 1. This system is somewhat reminiscent of a Van de Graaff generator. A boom out one side of the satellite contains an electron gun. This electron gun interacts with the ambient plasma and expels a beam of electrons. The electrons are given enough energy to "escape" the satellite system. The loss of electrons causes a net positive charge to build up on the craft. A conductive sphere is placed around the main spacecraft bus to hold this charge. The inside of the sphere will be neutral and have no electric fields, allowing the main satellite systems to operate normally. The spherical shell can be a lightweight, inflatable structure. If the shell's material is transparent, a solar power system can operate normally inside. Also, the communications subsystem of the spacecraft can be placed out on the boom to avoid interference due to the large potential of the satellite.

However, this system is limited in the charge it can produce. As charge builds up on the spherical surface, a negative pressure develops as all of the like charges repel each other. Depending on the thickness and strength of the shell material, a maximum charge is reached and the sphere essentially explodes. Peck[8] develops an expression for this charge, and gives the following example: for a small 1kg satellite with an advanced material 3m spherical shell, a maximum charge to mass ratio, or $\frac{q}{m}$, of 0.03 C/kg can be obtained.

III. Equations of Motion

We derive various equations of motion for the LAO system. These equations can be made somewhat arbitrarily complex by allowing for more general magnetic field orientations and representations. We deal first with the simplified case of a single charged satellite in a dipole field that is not tilted with respect to the axis of rotation of the central body. This result is followed by a more general treatment of energy and angular momentum changes due to the Lorentz Force.

A. Equations of Motion in a Non-tilted Dipole Field

We derive equations of motion for a single charged satellite in an Earth-centered, inertial spherical coordinate frame in the presence on a non-tilted dipole magnetic field. The spherical frame is defined by radius r, colatitude angle ϕ, and azimuth from the x-direction θ. The magnetic field is defined by

$$\vec{B} = \frac{B_0}{r^3}[2\cos\phi\hat{r} + \sin\phi\hat{\phi} + 0\hat{\theta}] \tag{2}$$

The field rotates fixed to the Earth. In the non-tilted field case, r and ϕ are equivalent in both the rotating field frame and the inertial frame. As the dipole is axisymmetric, the magnetic azimuth is unimportant to the Lorentz force. Note that for the Earth specifically, the geographic North Pole is technically the magnetic South Pole, hence the north side of a compass needle is attracted to the geomagnetic south pole. As we desire a coordinate system that has geographic north in the z-direction, we will be working with a dipole field that is essentially flipped upside down. We will correct for this fact by using a B_0 term that is less than zero.

The acceleration in the inertial frame is given by

$$\vec{a} = \vec{F}/m = -\frac{\mu}{r^3}\vec{r} + \frac{q}{m}\vec{v}_r \times \vec{B} \tag{3}$$

where $\frac{q}{m}$ is the charge to mass ratio of the satellite in c/kg, and $\vec{v_r}$ is the velocity of the spacecraft with respect to the magnetic field. As the magnetic field is locked in a solid rotation with the Earth, this velocity is given by

$$\vec{v}_r = \vec{v} - \omega_E\hat{n} \times \vec{r} \tag{4}$$

where $\vec{v}$ is the absolute velocity of the craft, ω_E is the Earth's rotation rate, and $\hat{n}$ is a unit vector in the direction of the true north pole.

Working out the Lorentz force in the spherical, inertial frame yields

$$\vec{F}_L = \frac{q}{m}(\dot{\vec{r}} - \vec{\omega}_E \times \vec{r}) \times \vec{B} = q\left(\begin{bmatrix} \dot{r} \\ r\dot{\phi} \\ r\dot{\theta}\sin\phi \end{bmatrix} - \omega_E \begin{bmatrix} \cos\phi \\ -\sin\phi \\ 0 \end{bmatrix} \times \begin{bmatrix} r \\ 0 \\ 0 \end{bmatrix}\right) \times \frac{B_0}{r^3}\begin{bmatrix} 2\cos\phi \\ \sin\phi \\ 0 \end{bmatrix} \tag{5}$$

which reduces to

$$\vec{F}_L = \frac{q}{m}\frac{B_0}{r^3}\begin{bmatrix} -r\dot{\theta}\sin^2\phi + \omega_E r\sin^2\phi \\ 2r\dot{\theta}\sin\phi\cos\phi - 2\omega_E r\cos\phi\sin\phi \\ \dot{r}\sin\phi - 2r\dot{\phi}\cos\phi \end{bmatrix} \tag{6}$$

Combining the Lorentz term with gravity and the standard accelerations in spherical coordinates gives the following three equations of motion:

$$\ddot{r} = r\dot{\theta}^2\sin^2\phi + r\dot{\phi}^2 - \frac{\mu}{r^2} - \frac{q}{m}\frac{B_0}{r^3}[r\dot{\theta}\sin^2\phi - \omega_E r\sin^2\phi] \tag{7}$$

$$r\ddot{\phi} = -2\dot{r}\dot{\phi} + r\dot{\theta}^2\sin\phi\cos\phi + \frac{q}{m}\frac{B_0}{r^3}2[r\dot{\theta}\sin\phi\cos\phi - \omega_E r\cos\phi\sin\phi] \tag{8}$$

$$r\ddot{\theta}\sin\phi = -2\dot{r}\dot{\theta}\sin\phi - 2r\dot{\phi}\dot{\theta}\cos\phi + \frac{q}{m}\frac{B_0}{r^3}[\dot{r}\sin\phi - 2r\dot{\phi}\cos\phi] \tag{9}$$

These three equations represent a sixth order system that applies to any orbit of a charged satellite in a non-tilted, dipole magnetic field.

B. General Energy and Angular Momentum Change

The work-energy principle gives

$$\dot{E} = \vec{v}\cdot\vec{F} \tag{10}$$

where E is the total energy of the system per unit mass, F is the applied force per unit mass, and v is the craft velocity. Including the Lorentz force gives:

$$\dot{E} = \vec{v}\cdot\left(\frac{q}{m}\vec{v}_r\times\vec{B}\right) \tag{11}$$

where $\vec{v_r}$ is given by Eq. 4. Applying this definition gives

$$\dot{E} = \vec{v}\cdot\left(\frac{q}{m}\vec{v}\times\vec{B}\right) - \vec{v}\cdot\left[\frac{q}{m}(\omega_E\hat{n}\times\vec{r})\times\vec{B}\right] \tag{12}$$

The $\vec{v}\cdot(\vec{v}\times\vec{B})$ term is zero, yielding

$$\dot{E} = \frac{q}{m}\vec{v}\cdot\left[\vec{B}\times(\omega_E\hat{n}\times\vec{r})\right] \tag{13}$$

This result shows that only the rotation of the magnetic filed allows the Lorentz Force to do work on the satellite. A general magnetic force is conservative, thus the change in energy comes not from the magnetic field, but from the rotation of the Earth. Some prefer to visualize that if a magnetic field in rotating it must be driven by an electric field, and this implied electric field can do work on a satellite.

Applying the triple cross product identity, $\vec{A}\times[\vec{B}\times\vec{C}] = \vec{B}(\vec{A}\cdot\vec{C}) - \vec{C}(\vec{A}\cdot\vec{B})$, to Eq. 13 gives the following equation:

$$\dot{E} = \frac{q}{m}\omega_E\left[(\vec{v}\cdot\hat{n})(\vec{B}\cdot\vec{r}) - (\vec{v}\cdot\vec{r})(\hat{n}\cdot\vec{B})\right] \tag{14}$$

This result is general, and applies for any orbit or magnetic filed configuration.

We can look at changes in the angular momentum in a similar way, by examining the torques applied to the system by the Lorentz Force, or

$$\dot{\vec{h}} = \vec{r}\times\vec{F} = \vec{r}\times\left(\frac{q}{m}\vec{v}_r\times\vec{B}\right) \tag{15}$$

where h is the angular momentum per unit mass of the system. Inserting our expression for v_r and simplify gives

$$\dot{\vec{h}} = \vec{r}\times\left(\frac{q}{m}\vec{v}\times\vec{B}\right) + \vec{r}\times\left(\vec{B}\times\left[\frac{q}{m}\omega_E\hat{n}\times\vec{r}\right]\right) \tag{16}$$

Applying the triple cross product formula to both terms and further simplifying yields the following general expression:

$$\dot{\vec{h}} = \frac{q}{m}(\vec{B}\cdot\vec{r})\vec{v} - \frac{q}{m}(\vec{r}\cdot\vec{v})\vec{B} - \frac{q}{m}\omega_E(\vec{B}\cdot\vec{r})(\hat{n}\times\vec{r}) \tag{17}$$

Depending on the orbital and magnetic configurations, we may change both the magnitude and direction of the angular momentum vector. Changing the direction of this vector will allow some measure of control over both the inclination and right ascension angle of the orbit. This control will be examined in more detail for two cases in the following section.

IV. Applications

Using the Lorentz Force in a beneficial way is sometimes not an intuitive exercise. The LAO system cannot control the the direction of the force, only magnitude and perhaps the sign, depending the implementation architecture. The force is also perpendicular to the velocity of the spacecraft with respect to the magnetic field. Were the magnetic field not rotating, no energy could be added to an LAO. But with the rotating field, the energy and angular momentum of the orbit can be changed in most cases. And with smart control of the charge on the satellite, controlling energy and momentum allows for control over most of the orbital elements of the spacecraft. Two specific cases will be developed below: the polar circular orbit and the general equatorial orbit, both in a non-tilted dipole field.

A. Polar Circular Orbit, Non-tilted Dipole Field

We can apply the general energy and momentum relationships developed earlier to two specific cases to develop some simple and interesting results. First we examine a polar circular orbit in a non-tilted dipole magnetic field. In this case the following expressions are true:

$$\vec{v}\cdot\vec{r}=0; \quad \vec{B}\cdot\vec{r}=2\frac{B_0}{r^2}\sin u; \quad \vec{v}\cdot\hat{n}=v_c\cos u; \quad v_c=\sqrt{\frac{\mu}{r}} \tag{18}$$

where r is the radius of the orbit, and u is the argument of latitude of the satellite. The argument of latitude is the angular position of the satellite around the orbit measured from the right ascension of the craft in the equatorial plane. Using these results in Eq. 14 gives

$$\dot{E}=2\frac{q}{m}\omega_E B_0\sqrt{\mu}r^{-5/2}\sin u\cos u \tag{19}$$

This expression is an odd, periodic function and, thus, contributes no secular change to the energy of the orbit. However, the radius of the orbit will undergo an oscillation with a frequency of twice per orbit. For any elliptical orbit, the total orbital energy can be expressed as a function of the semimajor axis:

$$E=-\frac{\mu}{2a} \tag{20}$$

where a is the semimajor axis, and in the circular case $a=r$. Differentiating this expression to find the change in radius with respect to energy gives

$$\dot{r}=2\frac{r^2}{\mu}\dot{E} \tag{21}$$

Using this equation and Eq. 19 gives a radius change throughout the orbit of

$$\dot{r}=4\frac{q}{m}\omega_E\frac{B_0}{\sqrt{\mu}}r^{-1/2}\sin u\cos u \tag{22}$$

For constant $\frac{q}{m}$, this expression is periodic, but we can control the charge as a function of the argument of latitude and create a secular change in the radius (and energy) of the orbit.

Similarly, the angular momentum change of a circular polar LAO is examined using Eq. 17, with the following relationships

$$\vec{r}\cdot\vec{v}=0; \quad \vec{B}\cdot\vec{r}=2\frac{B_0}{r^2}\sin u; \quad \vec{v}=\begin{bmatrix}-v_c\sin u\\ v_c\cos u\\ 0\end{bmatrix} \tag{23}$$

where the circular speed of the orbit is given by v_c, and, in the last expression, an orthogonal coordinate system has been assumed with the x-direction along the line of nodes, the y-direction aligned with the north pole, and the z-direction accordingly along the orbit angular momentum vector. This coordinate frame also gives

$$\hat{n}=\begin{bmatrix}0\\1\\0\end{bmatrix}; \quad \vec{r}=r\begin{bmatrix}\cos u\\ \sin u\\ 0\end{bmatrix}; \quad \hat{n}\times\vec{r}=r\begin{bmatrix}0\\0\\-\cos u\end{bmatrix} \tag{24}$$

Using all of these expressions in Eq. 17 and simplifying gives

$$\dot{\vec{h}} = 2\frac{q}{m}\frac{B_0}{r^2}\begin{bmatrix} -v_0 \sin^2 u \\ v_0 \sin u \cos u \\ r\omega_E \sin u \cos u \end{bmatrix} \tag{25}$$

which represents the time rate of change of the angular momentum vector due to the Lorentz force.

We use this vector derivative to define several scalar derivatives of interest, including the time rates of change of the inclination angle, the right ascension angle, and the magnitude of the angular momentum. First, the derivative of the scalar angular momentum magnitude is given by

$$\dot{h} = \dot{\vec{h}} \cdot \hat{h} = \dot{\vec{h}} \cdot \begin{bmatrix} 0 \\ 0 \\ 1 \end{bmatrix} \tag{26}$$

as our coordinate system has the initial angular momentum in the z-direction. This expression simplifies to

$$\dot{h} = 2\frac{q}{m}\frac{B_0}{r}\omega_E \sin u \cos u \tag{27}$$

Thus, the magnitude of the angular momentum vector changes solely in a periodic manner under a constant charge.

The inclination i angle is defined in terms of the angular momentum vector $\vec{h}$ by

$$\hat{n} \cdot \vec{h} = h \cos i \tag{28}$$

Differentiating this expression to find the time rate of change of i gives

$$\hat{n} \cdot \dot{\vec{h}} = \dot{h} \cos i - h \sin i \frac{di}{dt} \tag{29}$$

where the notation $\frac{di}{dt}$ is used for clarity. Solving for $\frac{di}{dt}$ and substituting in for the derivatives of angular momentum gives the following expression for time rate of change of inclination:

$$\frac{di}{dt} = \frac{-2\frac{q}{m}\frac{B_0}{r^2} \sin u \cos u \left[v_0 - r\omega_E \cos i\right]}{r v_0 \sin i} \tag{30}$$

Again, this is a nonsecular derivative for a constant charge changing a frequency of twice per orbit.

The line of nodes vector $\vec{\Omega}$ is defined by

$$\vec{\Omega} = \hat{n} \times \vec{h} \tag{31}$$

and is vector from the origin of the coordinate system through the point where the satellite ascends through the equatorial plane. Differentiating the $\vec{\Omega}$ gives

$$\dot{\vec{\Omega}} = \hat{n} \times \dot{\vec{h}} \tag{32}$$

which simplifies to

$$\dot{\vec{\Omega}} = \frac{2qB_0}{mr^2} v_0 \sin^2 u \begin{bmatrix} 0 \\ 0 \\ 1 \end{bmatrix} + \frac{2q\omega_E B_0}{mr} \sin u \cos u \begin{bmatrix} 1 \\ 0 \\ 0 \end{bmatrix} \tag{33}$$

There are two terms in this derivative, one along the direction of the node vector, and one normal to it. The length of the node vector is irrelevant in this situation. The term normal to the node vector is more interesting. It is in the equatorial plane, and thus represents a change in the right ascension angle. This term is an even function and produces a secular change. We can substitute into this expression the fact that the magnitude of the velocity in the circular orbit, v_c, is given by $r\dot{u}$. Thus the normal component of the vector right ascension change is

$$\dot{\vec{\Omega}}_n = \frac{2qB_0}{mr} \sin^2 u \dot{u} \tag{34}$$

We can relate this to the actual angular right ascension change, $\dot{\Omega}$, by

$$\dot{\Omega} = \frac{\|\dot{\vec{\Omega}}_n\|}{\|\vec{\Omega}\|} \tag{35}$$

In this polar case, the magnitude of the node vector is simply the magnitude of the angular momentum vector, or

$$\|\vec{\Omega}\| = \|\vec{h}\| = r\sqrt{\frac{r_0}{\mu}} \tag{36}$$

because the angular momentum is perpendicular to the north direction. Our expression becomes

$$\dot{\Omega} = 2\frac{q}{m}\frac{B_0}{r^2}\sqrt{\frac{r}{\mu}}\sin^2 u\dot{u} \tag{37}$$

This expression represents the change in right ascension angle as a function of argument of latitude. Once again, we note that this expression will produce a secular change in the right ascension angle for a constant charge.

We can determine an average change in right ascension per orbit by integrating Eg. 37 around one complete orbit. The change in right ascension per orbit $\Delta\Omega$ is given by

$$\Delta\Omega = 2\frac{q}{m}\frac{B_0}{r^2}\sqrt{\frac{r}{\mu}}\int_0^{2\pi} sin^2 u\ du \tag{38}$$

which easily yields the following simple expression for change in right ascension per orbit:

$$\Delta\Omega = 2\pi\frac{q}{m}\frac{B_0}{r^2}\sqrt{\frac{r}{\mu}} \tag{39}$$

Thus, for the circular polar orbit, non-tilted dipole case, we can set an arbitrary change in right ascension per orbit. We can relate this to an average right ascension Ω_{avg} change by multiplying by the period of the orbit:

$$\Delta\Omega = \Omega_{avg}\left(2\pi\sqrt{\frac{r^3}{\mu}}\right) \tag{40}$$

Using this expression in Eq. 39 gives the following simple relationship between the charge to mass ratio $\frac{q}{m}$ and the average right ascension rate Ω_{avg}, circular orbit radius r, and magnetic field strength B_0:

$$\frac{q}{m} = \frac{\dot{\Omega}_{avg}r^3}{B_0} \tag{41}$$

We can now calculate the necessary charge to mass ratio for any desired right ascension rate.

Changing the right ascension of a polar orbit essentially amounts to changing longitude on the ground track of the satellite. Thus, arbitrary right ascension control can greatly increase the efficiency of a polar LEO imaging satellite. If full charge control is possible (both positive and negative charges) then the satellite can acquire a target faster, and then stay in the neighborhood of the target longer. In fact, if an average right ascension rate equal to the rate of Earth's rotation is acquired, then a satellite can have a single-orbit repeat groundtrack. The craft would pass over exactly the same points on the Earth every orbit. Thus, the orbit becomes a LEO GT-1 orbit. This groundtrace would allow for an satellite to pass over an imaging target every 90 minutes rather than twice a day for an uncontrolled LEO polar satellite.

Solving for the required charge to mass ratio for an LAO GT-1 yields

$$\left(\frac{q}{m}\right)_{GT-1} = \frac{\omega_E r^3}{B_0} \tag{42}$$

When evaluated for a circular orbit with 400km altitude, a $\frac{q}{m}$ of -2.831 C/kg is required for geosynchronous behavior, the negative sign do the fact that B_0 is negative. This $\frac{q}{m}$ ratio is well above the maximum limit for the simple architecture presented above, but it is not out of the realm of future possibilities.

Another possible application is a sun synchronous LEO polar orbit at any altitude. The sun synchronous condition is a right ascension rate of $\dot{\Omega}_{ss} = 2\pi$ rad/year. As above, this yields a charge to mass ratio for maintaining a sun synchronous orbit of

$$\left(\frac{q}{m}\right)_{ss} = \frac{\dot{\Omega}_{ss} r_0^3}{B_0} \tag{43}$$

which for a 400km orbit evaluates to -0.0078 C/kg. This charge to mass ratio should be more easily obtainable with a simple architecture.

B. Equatorial Orbit, Non-tilted Dipole Field

A second simple case to consider is an equatorial orbit in a not-tilted dipole field. The true equator and the magnetic equator are aligned in this situation, and magnetic field is perpendicular to these planes. The eccentricity can be non-zero in this case.

The following relationships hold for this case:

$$\vec{v} \cdot \vec{n} = 0; \vec{B} \cdot \hat{n} = -\frac{B_0}{r^3}; \vec{r} \cdot \vec{v} = \sqrt{\mu a(1-e^2)} \frac{e \sin\nu}{1 + e\cos\nu} \tag{44}$$

where a is the orbit semimajor axis, e is the orbital eccentricity, and ν is the true anomaly. Using these expressions, and the standard conic section equation for an elliptical orbit

$$r = \frac{a(1-e^2)}{1 + e\cos\nu} \tag{45}$$

in Eq. 14 gives

$$\dot{E} = \frac{q}{m} \omega_E B_0 \sqrt{\mu} \left[a(1-e^2)\right]^{-5/2} e \sin\nu (1 + e\cos\nu)^2 \tag{46}$$

Note the dependence on the eccentricity e. A circular orbit can have no energy added by the method. Differentiating the equation given in Eq. 20 gives a time rate of change of semimajor axis of

$$\dot{a} = 2\frac{q}{m} e a^2 \omega_E \frac{B_0}{\sqrt{\mu}} \left[a(1-e^2)\right]^{-5/2} \sin\nu (1 + e\cos\nu)^2 \tag{47}$$

Again, this is a nonsecular change, but with proper control of $\frac{q}{m}$, the size of the equatorial orbit can be controlled using the Lorentz force.

Following the same procedure we can work out the angular momentum change for the equatorial orbit. Using these relationships:

$$\vec{B} \cdot \vec{r} = 0; \vec{B} = \frac{B_0}{r^3} \begin{bmatrix} 0 \\ 0 \\ -1 \end{bmatrix} \tag{48}$$

with $\vec{h}$ in the z-direction, with Eq. 17 gives

$$\dot{\vec{h}} = -\frac{q}{m} (\vec{r} \cdot \vec{v}) \frac{B_0}{r^3} \begin{bmatrix} 0 \\ 0 \\ -1 \end{bmatrix} \tag{49}$$

As this is only in the z-direction, it represents only a change in the scalar magnitude of $\vec{h}$:

$$\dot{h} = \frac{q}{m} \frac{B_0}{r^3} (\vec{r} \cdot \vec{v}) \tag{50}$$

Inserting our expressions for $r(\nu)$ and $\vec{r} \cdot \vec{r}$ gives

$$\dot{h} = \frac{q}{m} B_0 \sqrt{mu} \left[a(1-e^2)\right]^{-5/2} e \sin\nu (1 + e\cos\nu)^2 \tag{51}$$

which is another periodic function with no secular terms. Also, the direction of h cannot be controlled, which means the inclination and right ascension angle cannot be changed.

We can derive the change in orbital eccentricity based on the following equation given by Burns:[12]

$$\dot{e} = \frac{1}{2e}(e^2 - 1)\left[\frac{2\dot{h}}{h} + \frac{\dot{E}}{E}\right] \tag{52}$$

Applying our expressions for orbital energy and angular momentum change in Eqs. 46 and 51, respectively, gives

$$\dot{e} = -\frac{q}{m}B_0\frac{\sin\nu(1+e\cos\nu)^2}{[a(1-e^2)]^{3/2}}\left[\frac{1}{a^{3/2}(1-e^2)^{1/2}} - \frac{\omega_E}{\sqrt{\mu}}\right] \tag{53}$$

which is periodic over true anomaly. Note that we can change the eccentricity of an initially circular orbit. So if we start with an initially circular orbit we first change the eccentricity and the change the energy. Also from Burns,[12] we develop an expression for change in the argument of perigee, ω, using the equation:

$$\dot{\omega} = \dot{\theta} + (r^{-1} - \frac{E}{e\mu}\cos\nu)\frac{2h\dot{h}}{e\mu\sin\nu} - \frac{h^2}{(e\mu)^2}\dot{E}\cot\nu \tag{54}$$

where the term

$$\dot{\theta} = \cos(i)\dot{\Omega} = 0 \tag{55}$$

is zero because the direction of the angular momentum cannot change, and thus Ω is fixed. Again applying Eqs. 46 and 51 gives

$$\dot{\omega} = \frac{\frac{q}{m}B_0(1+e\cos\nu)^2}{[a(1-e^2)]^{3/2}}\left[2\frac{1+e\cos\nu}{[a(1-e^2)]^{3/2}} + \frac{\cos\nu}{a^{3/2}e(1-e^2)^{1/2}} - \frac{\omega_E\cos\nu}{e\sqrt{\mu}}\right] \tag{56}$$

Note that the first term in brackets of this equation gives rise to a secular change in the argument of perigee for a constant charge to mass ratio. This secular perigee change has many interesting, if somewhat esoteric, applications. Perigee control should allow for the cancelation of various natural perturbation on the argument od perigee, such as J2 effects and lunar and solar tides. Another use may be to create a Molniya-type orbit at zero inclination (and most likely other inclinations). Building on the same ideas as the GT-1 LAO orbits discussed above, we could control the average change in perigee not only cancel out natural perturbation, but also to match the Earth's rotation. This would create an orbit whose perigee and apogee would remain at a constant longitude on Earth's surface. Thus, LAO creates possibilities for other kinds of synchronous orbits rather than just GT-x orbits.

We want an expression for the $\frac{q}{m}$ necessary to generate a certain average perigee change. First, we recognize that

$$\dot{\nu} = \frac{\sqrt{\mu}(1+e\cos\nu)^2}{[a(1-e^2)]^{3/2}} \tag{57}$$

by differentiating Eq. 45 and applying conservation of momentum. Substituting this expression into Eq. 56 gives

$$\frac{d\omega}{dt} = \frac{\frac{q}{m}B_0}{\sqrt{mu}}\left[\frac{2}{[a(1-e^2)]^{3/2}} + \frac{2e\cos\nu}{[a(1-e^2)]^{3/2}} + \frac{\cos\nu}{a^{3/2}e(1-e^2)^{1/2}} - \frac{\omega_E\cos\nu}{e\sqrt{\mu}}\right]\frac{d\nu}{dt} \tag{58}$$

To find the change in perigee over one orbit, we cancel the dt from each side of the equation and integrate both sides, varying ν from 0 to 2π. The integral over 2π for all terms that depend solely on $\cos\nu$ will be zero leaving only

$$\Delta\omega = \frac{4\pi\frac{q}{m}B_0}{\sqrt{\mu}\,[a(1-e^2)]^{3/2}} \tag{59}$$

For a certain desired argument of perigee rate $\dot{\omega}_{des}$ we require that $\Delta\omega/\Delta t = \dot{\omega}_{des}$, where we set Δt to be one orbital period. Setting the resulting expression for $\Delta\omega$ equal to Eq. 59 and solving for $\frac{q}{m}$ gives a required charge to mass ration for some desired rate of perigee change:

$$\frac{q}{m} = \frac{\dot{\omega}_{des}a^3(1-e^2)^{3/2}}{2B_0} \tag{60}$$

This equation has similar dependencies as Eq. 41, the charge to mass required for a particular right ascension change for a polar circle. However, in the equatorial case, the eccentricity plays an important role in the

magnitude of charge required. A higher eccentricity corresponds to a higher velocity at perigee for a given orbit size, which makes a more effective use of the Lorentz force, allowing for a smaller charge to mass ratio. Equation 60 applies for any desired rate of change for argument of perigee. This includes mitigating oblateness and third-body effects as well as introducing synchronous behavior. However, as larger rates are required, the predicted $\frac{q}{m}$ will be less accurate. The derivation of the expression assumes that all the other orbital elements are changing slowly, and this may not be the case with a large charge to mass ratio.

V. Numerical Simulation

A numerical simulation is developed to test several of the above results. The simulation is an integration of the sixth-order system defined by Eqs. 7-9, performed by MATLAB©. It is valid for any orbit for a charged satellite in a non-tilted dipole field. The results of three different situations are presented here. First, a polar, circular orbit is calculated, using the charge to mass ratio calculated for GT-1 orbit. Second, an elliptical, equatorial orbit is integrated with constant charge. Third, an elliptical, equatorial orbit is simulated with an alternating polarity charge, designed to increase the orbital energy of the satellite in a secular manner. Table 1 shows the set of physical parameters common to all simulations.

Table 1. Initial conditions for polar, circular integration.

Parameter	Value
ω_E	7.272e-5 rad/s
μ	3.986e14 m^3/s^2
B_0	-8.000e15 Wb-m

A. Polar Circular Orbit

The polar circular integration is calculated using the initial conditions in Table 2. The charge to mass ratio of 2.831 is chosen based on Eq. 42. Figure 2 shows the resulting orbital path. This path is plotted in a frame

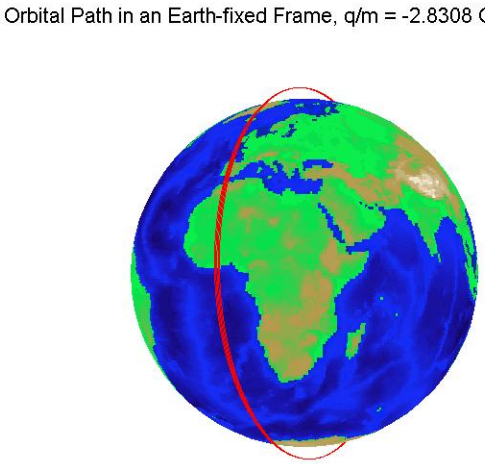

Figure 2. Track of a GT-1 LAO orbit in a frame rotating with Earth.

that rotates with the Earth, so as to highlight the GT-1 nature of the orbit. The orbit is properly scaled with the image of the Earth. When Fig. 2 is closely examined, we notice that orbit does slightly drift away from a perfect GT-1 orbit. This discrepancy can be explained by Fig. 3. This figure shows a comparison of

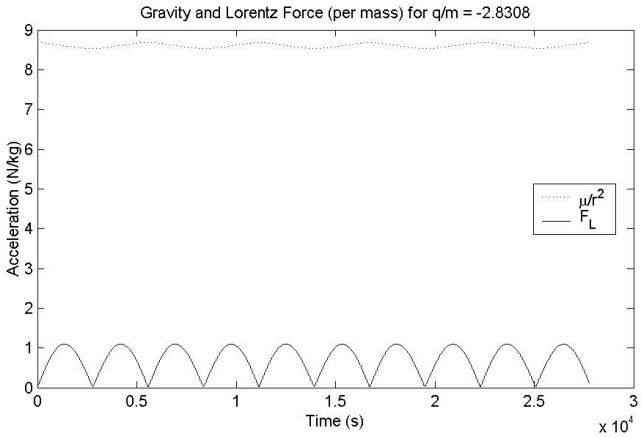

Figure 3. Comparison between gravitational and Lorentz force magnitudes for a GT-1 LAO orbit.

the forces acting on the satellite. The magnitudes of both gravity and experienced Lorentz force are shown. In this GT-1 polar scenario, we see that the Lorentz force is quite significant with respect to gravity, and this causes some perturbations that erode earlier assumptions. A large Lorentz force will cause the orbital eccentricity to be non-zero, create wobbles in the inclination, and keep the orbital speed from being constant. These perturbations on the orbit will cause slight inaccuracies in the expressions derived above related to a polar circular orbit.

Table 2. Initial conditions for polar, circular integration.

Property	**Value**
Altitude	400 km
$\frac{q}{m}$	-2.831 C/kg
Integration Time	5 orbits

However, the small difference in calculated and desired right ascension angles is only due to wind up of small errors in predicted right ascension rate over time. Figure 4 show both the numerically calculated and the analytically derived right ascension angle rates. The analytical results are based on the expression in Eq. 37; the numerical result is based upon changes in the angular momentum vector of the orbit determined from the state of the system at any given time. These two expressions match nearly exactly, with extremely small, but persistent, errors. As expected, the right ascension rate is zero as the satellite crosses the equator, and large and negative as it crosses the poles. Note that the average values of these expression is less than zero, causing a secular decrease in the right ascension of the orbit. This decrease is easily seen in Fig. 5, which presents the calculated right ascension angle. These values are produced using the direction of the angular momentum of the orbit, calculated at each time step.

Finally, Fig. 6 shows the time rate of change of orbital energy throughout the simulation. The solid line represents the numerically calculated energy change based on the state vector at each time, and the dotted line represents the derived expression shown in Eq. 19. These two curves match closely. However, the energy change is centered around zero, and thus there is no secular change in the orbital energy.

B. Equatorial Orbit, Constant Charge

The equatorial, eccentric, constant charge simulation is initialized using the values shown in Table 3, using the same code base as the previous simulation. The chosen charge to mass ratio is designed to produce an Earth synchronous motion of the perigee of the orbit. The value is determined using Eq. 60 with a desired rotation rate designed to match the Earth's rotation, or $\dot{\omega}_{des} = -\omega_E$.

Figure 7 shows the orbital path of the satellite over five orbits. Again, the orbit is to scale with the

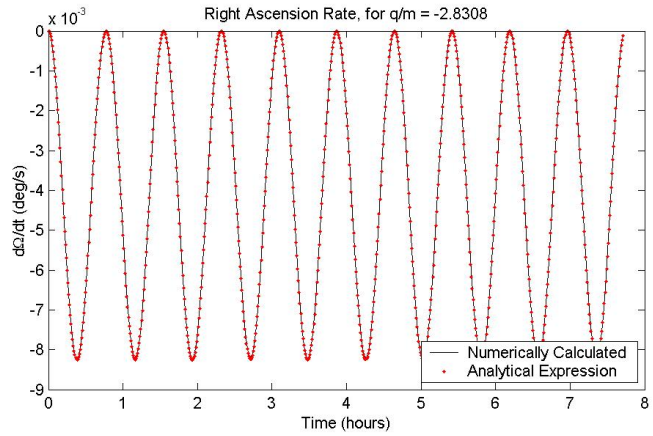

Figure 4. Right ascension time rate of change for a GT-1 LAO orbit.

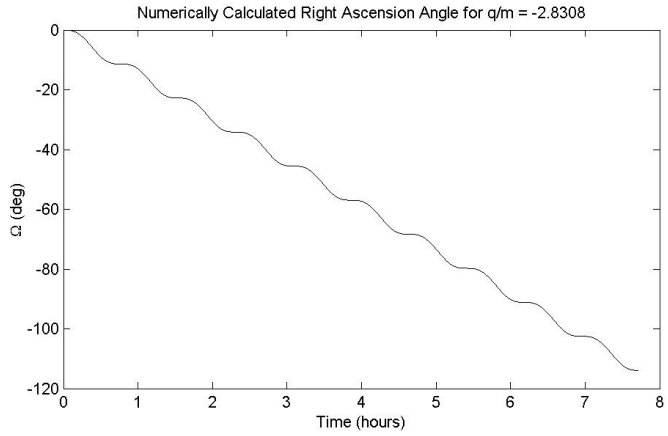

Figure 5. Right ascension angle of a GT-1 LAO orbit.

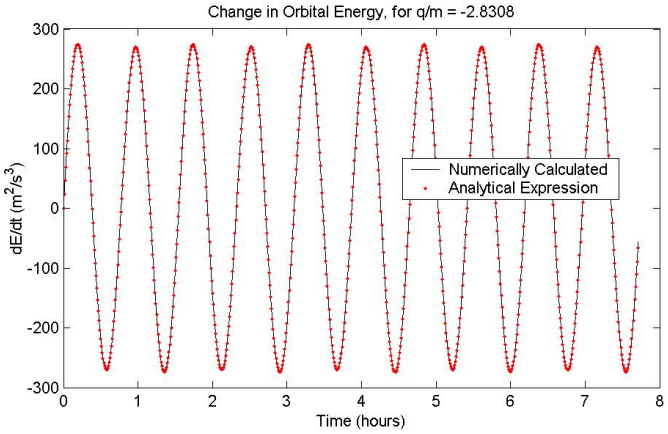

Figure 6. Time rate of change of orbital energy for a GT-1 LAO orbit.

Table 3. Initial conditions for equatorial, constant charge integration.

Property	Value
Perigee Altitude	400 km
Apogee Altitude	1500 km
Eccentricity	0.075
Semimajor Axis	7328 km
$\frac{q}{m}$	1.774 C/kg
Integration Time	1 day

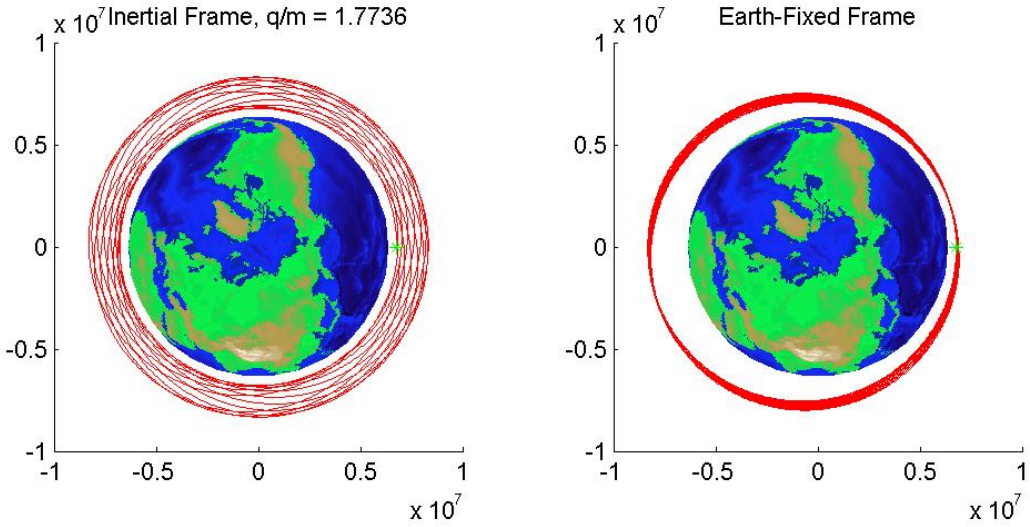

Figure 7. Orbital path of an equatorial, constant charge LAO satellite with $\frac{q}{m}$ calculated for synchronous perigee movement. The left figure shows the satellite's path in an inertial frame. The right image displays the track in a frame rotating with the Earth.

depiction of the Earth, the point of view here being looking down onto the North Pole. The track is shown in two different reference frames, the left being an inertial, non-rotating frames, and the right track shown in a frame that rotates with the Earth. The green star on this plot represents the starting point of the integration, which is at the initial perigee in this case.

The rotating frame view in Fig.7 show that the charge to mass ratio used in the simulation was not large enough to perfectly cancel the Earth's rotation with perigee motion. If the correct charge was used the rotating frame view would only show a single orbit. Figure 8 show the numerically calculated and analytically derived arguments of perigee for this case. The numerical values are represented by the solid line. The dotted represents the analytical values, calculated by numerically integrating Eq. 56. While these two curves match quite precisely, we see that the perigee angle does not reach 0° after one day as intended. The results of Fig. 8 give us confidence in the result for time rate of change of perigee expressed in Eq. 56, but show that accuracy is lost in integrating this result to obtain Eq. 60. In that integration, we assumed that the semimajor axis and eccentricity were changing slowly enough that we could assume the both a and e were not functions of true anomaly ν. However, the charge to mass ratios are large enough in this case to make that a poor assumption. However, for smaller desired perigee rate, like mitigating J2 effects, Eq. 60 is quite accurate. Creating the Earth synchronous effect is certainly possible, it just requires a larger $\frac{q}{m}$ than predicted.

The curves depicted in Fig. 9 represent the time rate of change of orbital energy for the LAO satellite. Again the numerical values are represented by a solid line, and are calculated based on the work done on the

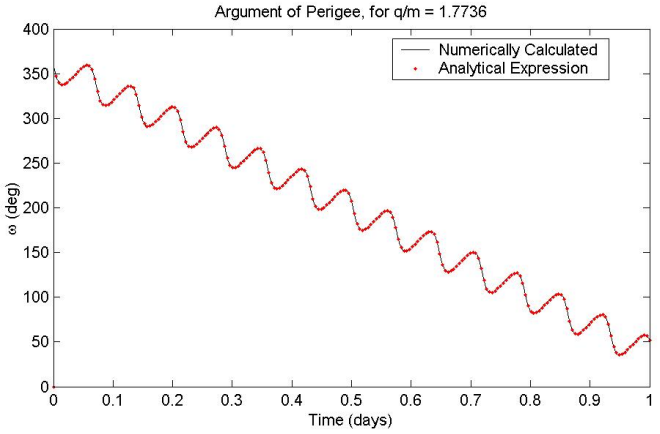

Figure 8. Perigee angle of an equatorial, constant charge LAO satellite.

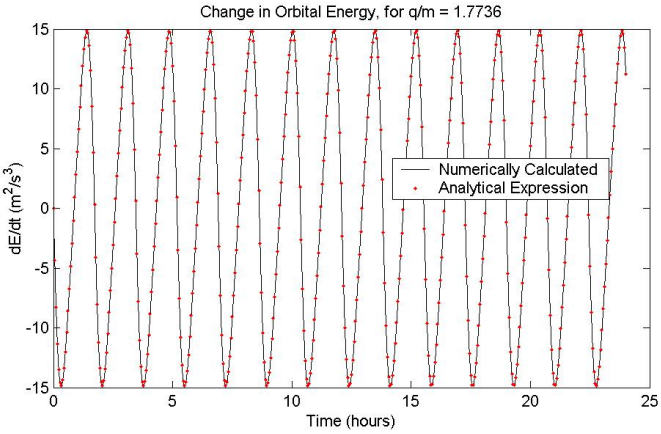

Figure 9. Time rate of change of orbital energy for an equatorial, constant charge LAO satellite.

satellite by the Lorentz force at any given time. The dotted curve shows the analytical result based on the expression in Eq. 46. These two curves agree nearly exactly, showing an energy change that is zero-mean. As expected, the largest change in E occur around perigee, with smaller effects near apogee.

Figure 10 shows changes in orbital eccentricity over the length of the simulation. The solid curve is a

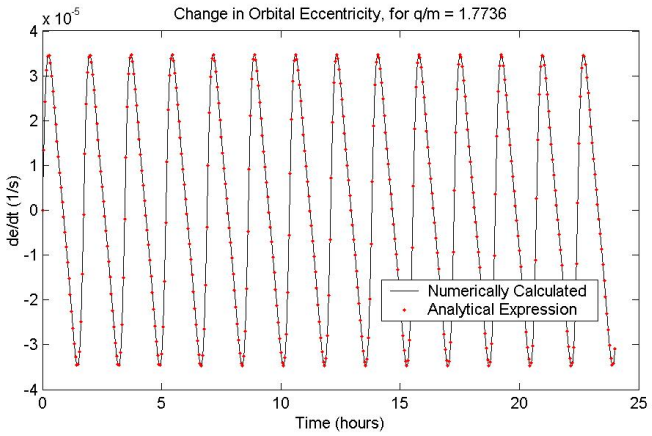

Figure 10. Time rate of change of orbital eccentricity for an equatorial, constant charge LAO satellite.

numerical differentiation of the eccentricity calculated at each time step. The dotted line is the result of applying Eq. 53. The results are well matched, zero-mean, and exhibit much larger changes around perigee than apogee.

Thus, we see that a constant charge, equatorial LAO satellite can have an arbitrary time rate of change of argument of perigee. The required charge to mass ratio for a desired rate depends solely on the initial orbit configuration and the magnitude of the desired change. The orbital energy and eccentricity also change in a predictable manner, but with no secular variations.

C. Equatorial Orbit, Alternating Polarity Charge

The final simulation presented here represents an attempt to use an extremely simple control of the satellite's charge to exploit the orbital energy changes seen above. By alternating the sign of the charge on the satellite in successive halves of the orbit, we can reverse the sign of the negative energy changes seen in Fig. 9 and cause a continued growth in the energy of the orbit. The initial conditions for this simulation are shown in Table 4. The charge to mass ratio listed in this table is simply the magnitude used throughout the

Table 4. Initial conditions for equatorial, constant charge integration.

Property	Value
Perigee Altitude	400 km
Apogee Altitude	35768 km
Eccentricity	0.723
Semimajor Axis	24462 km
$\frac{q}{m}$ Magnitude	3 C/kg
Integration Time	2 years

integration. From perigee to apogee, the charge is applied with a negative polarity, and, between apogee and perigee, a positive charge is maintained. This setup assumes that the craft can change the polarity of its charge instantly at the apses of the orbit. The orbital parameters are defined such the initial orbit is a geostationary transfer orbit, which represents an elliptical transfer orbit between LEO parking orbit and an orbit at geosynchronous altitude.

The resulting orbital path of the satellite over two years is presented in Fig. 11. This figure looks down

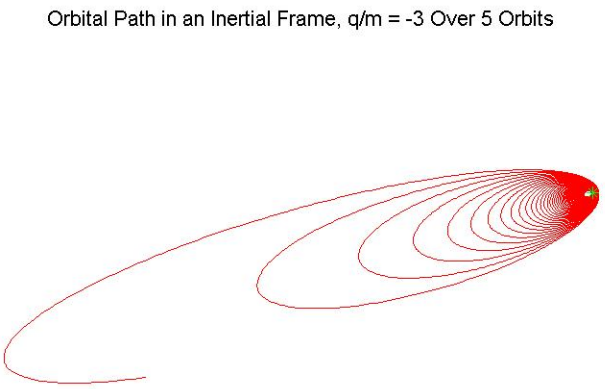

Figure 11. Orbital path of an alternating charge, equatorial LAO satellite in an Earth-centered inertial frame.

upon the Earth from the North Pole. The Earth is too small to be shown in this figure. Both the orbital energy and eccentricity continue to increase. By the end of the 2 year period the maximum distance from Earth achieved is over 3.4 million kilometers. We also note that this particular charge alternation scheme negates the secular changes in argument of perigee, in favor of secular changes in energy.

The orbital energy steadily approaches zero, as shown in Fig. 12. However, as most of the energy increase

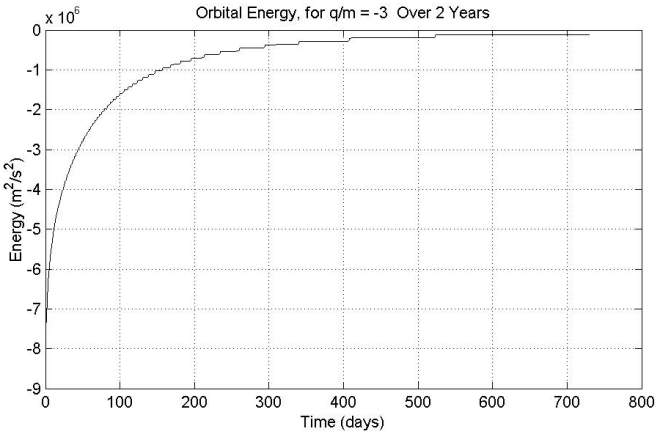

Figure 12. Orbital energy of an alternating charge, equatorial LAO satellite.

occurs around perigee, the rate of increase slows down as the energy increases. As the energy approaches zero, each orbit takes a longer time to complete, and thus each perigee passage occurs later. Although the orbital energy will eventually reach zero, this simulation is well past the point where third-body perturbations of the Sun and Moon would need to be considered.

These three simulations have shown excellent agreement between the derived equations of motion and the analytical expressions for the orbital changes created by the LAO system. We see that useful and desirable changes can be made to orbits using this system. Although simulations of only polar and equatorial orbits are presented here, an arbitrarily inclined orbit will just combine the properties of these two results in some way. While constantly charged satellites definitely exhibit interesting behavior, simple control schemes can

be used to greatly increase the capabilities of the LAO system. The simple alternating scheme applied above to the equatorial case can just as easily be applied to the polar case.

VI. Conclusion

Lorentz Augmented Orbits are based on simple physical principles but can be used to accomplish a variety complex orbital applications. Analytical results, tested by numerical simulations, show the effects that the Lorentz force has on the orbit of an LAO satellite. The resulting changes in orbital elements can be used to develop novel applications for the LAO system. These new application include polar, single orbit repeat groundtrack (GT-1) satellites. These orbits can exist at any altitude, not just the traditional GEO height. A successfully implement GT-1 LAO orbit would greatly outperform today's imaging satellites. Also numerically confirmed is the existence of equatorial orbits with arbitrary control over the location of perigee. These orbit can also create an Earth synchronous system, with the perigee and apogee of an orbit staying at a constant longitude on the surface of the Earth. The above applications rely on only maintaining a constant charge to mass ratio on the satellite; many further applications can be developed for fully controlling the charge based on the various expressions for orbital element change presented here.

Many avenues for future work exist within the LAO framework. The dynamics of the system based on a more complex and realistic model of the geomagnetic field will be examined. Also, the resulted printed here will be extended to arbitrary orbits rather than just polar and equatorial. The applications of LAO spacecraft to formation flight will also be examined in addition to further explorations of possible system architectures.

Acknowledgments

This work was supported by the NASA Institute for Advanced Concepts.

References

[1]Schaffer, L. and Burns, J. A., "The Dynamics of Weakly Charged Dust: Motion Through Jupiter's Gravitational and Magnetic Fields," *Journal of Geophysical Research*, Vol. 92, 1987, pp. 2264–2280.

[2]Schaffer, L. and Burns, J. A., "Charged Dust in Planetary Magnetospheres: Hamiltonian Dynamics and Numerical Simulations for Highly Charged Grains," *Journal of Geophysical Research*, Vol. 99, 1994, pp. 17211–17223.

[3]Mullen, E. G., Gussenhoven, M. S., and Hardy, D. A., "SCATHA Survey of High-Voltage Spacecraft Charging in Sunlight," *Journal of the Geophysical Science*, Vol. 91, 1986, pp. 1074–1090.

[4]Garrett, H. B. and Whittlesey, A. C., "Spacecraft Charging, An Update," *IEEE Transactions on Plasma Science*, Vol. 28, No. 6, 2000, pp. 2017–2028.

[5]Schaub, H., Parker, G. G., and King, L. B., "Challenges and Prospects of Coulomb Spacecraft Formations," *Proceedings of the AAS John L. Junkins Symposium*, May 2003.

[6]Lai, S. T., "An Overview of Electron and Ion Beam Effects in Charging and Discharging of Spacecraft," *IEEE Transactions on Nuclear Science*, Vol. 36, No. 6, 1989, pp. 2027–2032.

[7]Hough, M. E., "Lorentz Force Perturbations of A Charged Ballistic Missile," *Proceedings of the AIAA Guidance and Control Conference*, August 1982.

[8]Peck, M. A., "Prospects and Challenges ofr Lorentz-Augmented Orbits," *Proceedings of the AIAA Guidance, Navigation, and Control Conference*, August 2005.

[9]Schaub, H., "Stabilization of Ssatellite Motion Relative to a Coulomb Spacecraft Formation," *Journal of Guidance, Control, and Dynamics*, Vol. 28, No. 6, 2005, pp. 1231–1239.

[10]Kong, E., Kwon, D. W., Schweighart, S. A., Elias, L. M., Sedwick, R. J., and Miller, D. W., "Electromagnetic Formation Flight for Multisatellite Arrays," *Journal of Spacecraft and Rockets*, Vol. 41, No. 4, 2004, pp. 659–665.

[11]Tikhonov, A. A., "A Method of Semipassive Attitude Stabilization of a Spacecraft in the Geomagnetic Field," *Cosmic Research*, Vol. 41, No. 1, 2003, pp. 69–79.

[12]Burns, J. A., "Elementary derivation of the perturbation equations of celestial mechanics," *American Journal of Physics*, Vol. 44, No. 10, 1976, pp. 944–949.

Appendix B

Prospects for Lorentz Augmentation in Jovian Captures

Justin Atchison, Brett Streetman, and Mason A. Peck

To be presented at the 2006 AIAA GNC Conference

Prospects for Lorentz Augmentation in Jovian Captures

Justin A. Atchison*, Brett Streetman†, and Mason A. Peck‡
Cornell University, Ithaca, New York 14853

The Lorentz force is evaluated as a source of propellantless propulsion for capture into a Jovian orbit. Charged bodies orbiting Jupiter experience the greatest Lorentz force in the solar system, and therefore offers a strong proof-of-concept study for this novel technology. We model Jupiter's magnetosphere as an axis-aligned dipole and neglect perturbations such as planetary oblateness, third-body interferences, and drag. The charge is assumed to be constant in magnitude, but of variable polarity and/or bang-bang switching. Numerical simulations indicate that a capture is possible for a significant range of conditions, most importantly a switched, low charge-to-mass ratio that brings the satellite into Europa orbit within three years.

I. Introduction

Propellantless spacecraft propulsion opens up many new missions where launch cost, mass requirements, or the need for non-Keplerian orbital behaviors drive the mission design. This study explores the use of the Lorentz force as a novel means of propellantless planetary capture. The Lorentz force is experienced by a charged particle moving relative to a magnetic field. Maxwell's equations show that a time-varying magnetic field (a rotating planetary magnetosphere, for instance) is associated with an electric field. This electric field is the means by which work is done on the charged particle in an inertial frame[1].

While both the dynamics of a charged particle in a magnetic field (e.g. an electron beam in a cathode-ray tube) and the dynamics of body in a gravitational field are well understood, there is relatively little theory at the interface of the two. Typical satellites acquire charge by exposure to the near-earth space environment, but this charge is negligible, as is the resulting Lorentz force. However, recent results from the Voyager and Galileo missions have shown that the Lorentz force is a dominant perturbing force that is responsible for the non-equatorial halo in the ring structures around Jupiter (Fig. 1)[2,3]. This research inspires us to ask whether one can use this perturbing effect for orbit control by modulating a spacecraft's charge. In particular, we consider the application of Lorentz-force propulsion to the problem of efficient Jovian captures.

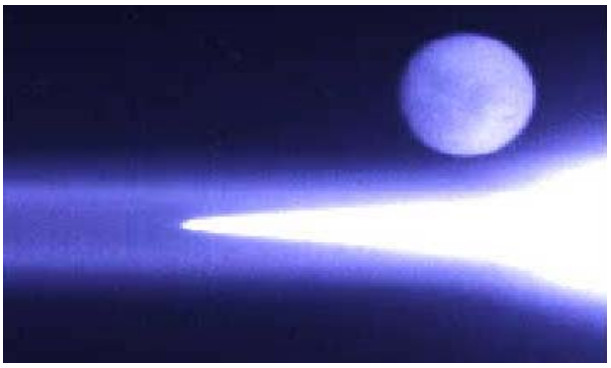

Figure 1. Structure of Jupiter's ring with Europa in rear. Courtesy NASA/JPL.

* Graduate Research Assistant, Sibley School of Mechanical and Aerospace Engineering, 245 Upson Hall, Student Member AIAA.
† Graduate Research Assistant, Sibley School of Mechanical and Aerospace Engineering, 245 Upson Hall, Student Member AIAA.
‡ Assistant Professor, Sibley School of Mechanical and Aerospace Engineering, 212 Upson Hall, Member AIAA.

II. Target Planet

Jupiter is in itself an appealing planet to study. It has and will be the target of numerous NASA missions including two that will launch within the next five years. JUNO will focus on identifying water content in Jupiter's core, and more importantly to our work: characterizing Jupiter's polar magnetic field. The New Horizons Probe will spend four months observing the Jovian system, including a detailed mapping of the Jovian magnetotail, a significant feature of the complex Jovian magnetosphere. Previous missions include two Pioneer fly-bys, both Voyager fly-bys, Galileo, Ulysses, and Cassini[4].

Further, the four primary moons of Jupiter are the center of scientific interest. Two missions have been conceptually designed to orbit Europa, measure the distribution of water ice and search for biological compounds. Jupiter Icy Moons Orbiter (JIMO) was cancelled, though it was initially planned to launch as soon as 2012.

Beyond this clear interest from the scientific community, Jupiter has two key features that identify it as an ideal target candidate for a Lorentz-capture maneuver. The first is that Jupiter has the highest rotation rate of the solar planets, 2.4 times that of Earth. The second element is a powerful magnetic field, both in terms of range and energy. Jupiter's magnetosphere is the largest planetary structure in the solar system, with a tail that extends beyond Saturn[4]. This field also contains a great deal of energy, roughly 20,000 times that of Earth's magnetosphere. These two characteristics make the Lorentz force most pronounced at Jupiter, thus making it the most practical planet at which to first evaluate Lorentz propulsion.

Jupiter's magnetosphere adds considerable complexity to efforts to model such a system. As of yet, no single model comprehensively describes the field, predominantly due to a lack of observational data[5]. The inner portions of the field (up to 4~6 Jovian equatorial radii, R_J) are generated by a thermo-convection-driven-dynamo near the surface of the planet. The middle portion of the field (4~6 to 30~50 R_J) is driven by an equatorial azimuthal current disc. This portion also directly interacts with Io, which is consequently a source of dusty plasma in Jupiter's rings. The most applicable model for this portion is an axis-aligned dipole field. The third region is a buffer zone that is characteristically non-symmetrical and experiences measurable changes on the order of hours in response to solar pressures and rotational effects. Finally, the outermost zone is the magnetotail which extends to as much as 200 R_J[6].

III. Derivations

A. Equations of Motion

We take the barycenter of the system to be located at Jupiter's center of mass. Spherical coordinates provide a set of basis vectors that conveniently describe the system: $\left(\hat{r},\hat{\phi},\hat{\theta}\right)$, where $\hat{r}$ is the unit vector in the radial direction, $\hat{\phi}$ is the unit vector in the polar angle direction, and $\hat{\theta}$ is the unit vector in the azimuthal direction. The Lorentz force is defined by

$$\mathbf{F_L} = q\,\mathbf{v_r} \times \mathbf{B} \tag{1}$$

where $\mathbf{F_L}$ is the Lorentz force experienced by the body with charge $\boldsymbol{q}$ and velocity $\boldsymbol{v_r}$ relative to Jupiter's magnetic field $\boldsymbol{B}$. This relative velocity is further defined by

$$\mathbf{v_r} = \frac{{}^N d}{dt}\mathbf{r} - \boldsymbol{\omega}_\mathbf{J} \times \mathbf{r} \tag{2}$$

where $\frac{{}^N d}{dt}\boldsymbol{r}$ is the vector time derivative in a Newtonian frame of $\boldsymbol{r}$, the position of the satellite, and $\boldsymbol{\omega_J}$ is the rotation rate of Jupiter. The magnetic field is modeled as a dipole aligned with Jupiter's angular velocity vector:

$$\mathbf{B} = \frac{-B_0}{r^3}\begin{pmatrix} 2\cos\phi \\ \sin\phi \\ 0 \end{pmatrix} \tag{3}$$

where B_0 is the dipole magnetic field strength at the magnetic equator ($r = R_J$). We have previously shown[7] that the Lorentz force can be represented as

$$\mathbf{F_L} = q\frac{B_0}{r^3}\begin{pmatrix} r\sin^2\phi\left(\dot{\theta}-\omega_J\right) \\ r\sin(2\phi)\left(\dot{\theta}-\omega_J\right) \\ 2r\dot{\phi}\cos\phi - \dot{r}\sin\phi \end{pmatrix} \tag{4}$$

Applying this force to Newton's equations of motion, using Newtonian gravity with μ as the mass of Jupiter times the gravitational constant, and substituting the vector accelerations in spherical coordinates yields the following equations of motion, in which the Lorentz acceleration has been normalized by collecting the term q/m as the satellite's characteristic charge-to-mass ratio:

$$\ddot{r} = r\dot{\phi}^2 + r\dot{\theta}^2\sin^2\phi - \frac{\mu}{r^2} + \frac{q}{m}\frac{B_0}{r^2}\sin^2\phi\left(\dot{\theta}-\omega_J\right) \tag{5}$$

$$\ddot{\phi} = \dot{\theta}^2\sin\phi\cos\phi - 2\frac{\dot{r}\dot{\phi}}{r} + \frac{q}{m}\frac{B_0}{r^2}\sin(2\phi)\left(\dot{\theta}-\omega_J\right) \tag{6}$$

$$\ddot{\theta} = \frac{1}{r\sin\phi}\left(-2\dot{r}\dot{\theta}\sin\phi - 2r\dot{\theta}\dot{\phi}\cos\phi + \frac{q}{m}\frac{B_0}{r^3}\left(2r\dot{\phi}\cos\phi - \dot{r}\sin\phi\right)\right) \tag{7}$$

For a magnetic equatorial model, the polar coordinate is set to $\phi = \pi/2$, reducing the system to two basis coordinates $\left(\hat{r},\hat{\theta}\right)$ and simplifying the equations of motion to

$$\ddot{r} = r\dot{\theta}^2 - \frac{\mu}{r^2} + \frac{q}{m}\frac{B_0}{r^2}\left(\dot{\theta}-\omega_J\right) \tag{8}$$

$$\ddot{\theta} = \frac{1}{r}\left(2\dot{r}\dot{\theta} - \frac{q}{m}\frac{B_0}{r^3}\dot{r}\right) \tag{9}$$

B. Perturbation Equations

The position and velocity of an elliptical orbit at the magnetic equator are given in terms of the classical orbital elements in Eq. 10 – 13. We have previously derived[7] perturbation equations for these orbital elements and characteristic quantities (Eq. 14 – 18). The orbital elements (a,e,ω,ν) are semi-major axis, eccentricity, argument of perigee, and true anomaly respectively. The total energy per unit mass E and the angular momentum per unit mass h are also shown to change as functions of these elements.

$$|r| = \frac{a\left(1-e^2\right)}{1+e\cos\nu} \tag{10}$$

$$|\dot{r}| = \sqrt{\frac{\mu}{a\left(1-e^2\right)}}\, e \sin \nu \tag{11}$$

$$|\dot{\nu}| = \frac{\sqrt{\mu}}{\left[a\left(1-e^2\right)\right]^{3/2}} \left(1+e\cos\nu\right)^2 \tag{12}$$

$$\nu = \theta - \omega \tag{13}$$

$$\dot{a} = 2\frac{q}{m}\frac{\omega_J B_0}{\sqrt{\mu}}\left[a\left(1-e^2\right)\right]^{-5/2} e\, a^2 \sin\nu \left(1+e\cos\nu\right)^2 \tag{14}$$

$$\dot{e} = -\frac{q}{m} B_0 \frac{\sin\nu\left(1+e\cos\nu\right)^2}{\left[a\left(1-e^2\right)\right]^{3/2}} \left[\frac{1}{a^{3/2}\left(1-e^2\right)^{1/2}} - \frac{\omega_J}{\sqrt{\mu}}\right] \tag{15}$$

$$\dot{\omega} = \frac{q}{m} B_0 \frac{\left(1+e\cos\nu\right)^2}{\left[a\left(1-e^2\right)\right]^{3/2}} \left[2\frac{1+e\cos\nu}{\left[a\left(1-e^2\right)\right]^{3/2}} + \frac{\cos\nu}{a^{3/2}\left(1-e^2\right)^{1/2}} - \frac{\omega_J \cos\nu}{e\sqrt{\mu}}\right] \tag{16}$$

$$\dot{E} = \frac{q}{m}\omega_J B_0 \sqrt{\mu}\left[a\left(1-e^2\right)\right]^{-5/2} e \sin\nu \left(1+e\cos\nu\right)^2 \tag{17}$$

$$\dot{h} = \frac{q}{m} B_0 \sqrt{\mu}\left[a\left(1-e^2\right)\right]^{-5/2} e \sin\nu \left(1+e\cos\nu\right)^2 \tag{18}$$

The contour plots shown in Fig. 2 show the trends of eccentricity and semi-major axis change over a range of orbits and charge-to-mass ratios. These plots offer the important insight that the eccentricity is the dominant factor in determining the change in eccentricity and semi-major axis. That is to say, the perturbations are significantly weaker in a circular orbit.

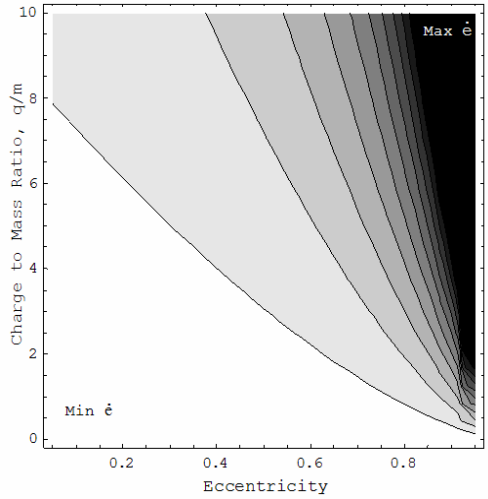

a.) Time derivative of e as a function of q/m and e.

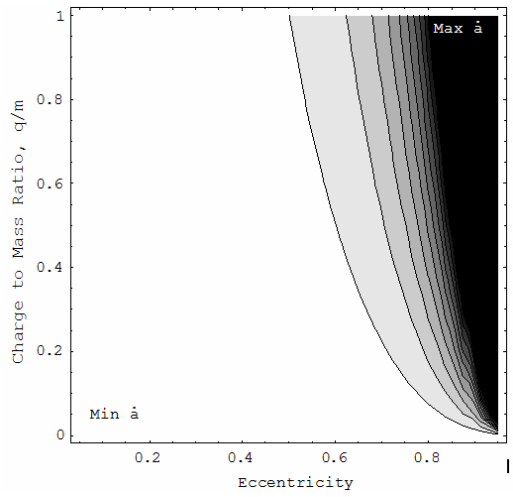

b.) Time derivative of a as a function of q/m and e.

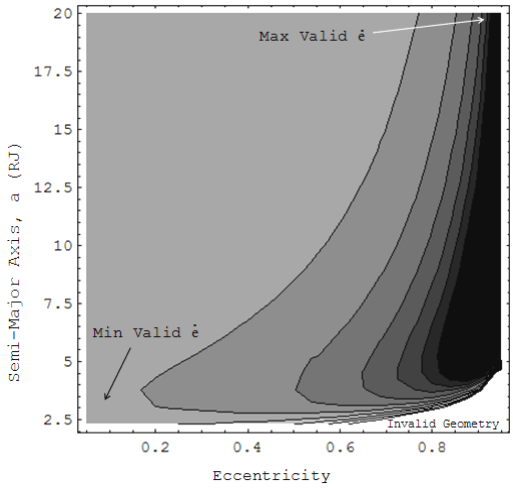

c.) Time derivative of e as a function of e and a.

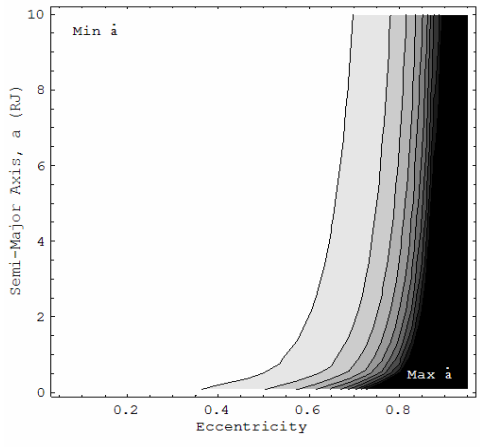

d.) Time derivative of a as a function of e and a.

Figure 2. Contour plots of the orbital perturbations (note inconsistent scales)

IV. Mission Description

The purpose of this study is to gain insight into the proposed mechanism of orbit evolution via the Lorentz force and to evaluate the feasibility of utilizing a spacecraft's charge to perturb an approaching satellite into a useful orbit around Jupiter. This scope includes finding a successful range of parameters associated with the satellite's charge, lifetime, controllability, and approach conditions that could reasonably compare to existing technologies.

A. Limitations

The magnetic field model only approximates the middle range of the magnetosphere, and neglects the other complex, evolving features. This range is important because it is best modeled by a relatively simple and well understood magnetic dipole tilted 9.5 ^{o}-10.8^{o} to the axis of rotation[6]. Our model neglects this tilt and aligns the field with Jupiter's axis of rotation. The range is also important because the four Galilean satellites are within this range (Io ~ 5.9 R_J to Calisto ~ 26 R_J), thus making it useful in terms of scientific interest.

The model also neglects perturbations associated with the Galilean satellites, planetary oblateness, or atmospheric drag. It also does not consider the effects of variable charge, plasma interaction, or power limitations. Rather, it considers the most simple case of a constant magnitude charge that can be alternated in polarity and/or switched on and off in a controlled manner.

B. Initial Conditions

For all of the simulated cases, we selected an initially parabolic orbit. Not only does this decision represent a "neutral" initial energy, but it reduces the input space to one degree of freedom, the initial perijove. Reviewing the data available from the NASA Space Science Data Center[§] in Table 1, three things are apparent. First, it is reasonable to consider an equatorial case, since the non-polar satellites had inclinations within the tilt of the magnetic dipole axis. Second, it is reasonable to use an initially parabolic approach since Galileo first approached Jupiter with a flyby eccentricity as low as 1.071. Finally, a perijove radius of 4.0 R_J is appropriate since Galileo orbited at this range. This value is also fitting because it serves as the lower range of the middle portion of the magnetosphere where the dipole model is valid.

[§] NASA Space Science Data Center Master Catalog. Goddard Space Flight Center, Greenbelt, MD http://nssdc.gsfc.nasa.gov/

Table 1. Previous Mission Parameters				
Mission	Purpose	Eccentricity, e	Perijove, r_p	Inclination, i
Pioneer 11	Flyby		1.6 R_J	51.8 deg
Voyager 1	Sensing	1.319	4.89 R_J	1.318 deg
Voyager 2	Flyby	1.330	10.11 R_J	6.913 deg
Galileo	Flyby	1.071	4.08 R_J	5.148 deg
Galileo	Orbit		4.01 R_J	
Ulysses	Flyby	1.66	6.3 R_J	154.6 deg

The second parameter is the initial radius. While it doesn't serve to define the orbit, it does act as an initial limit of integration. Based on the range of the middle magnetosphere, the upper limit of 50 R_J was selected. This combination yields the values given in Table 2.

Table 2. Initial Conditions for Simulation	
r	50 R_J
ν	147.1 deg
$\dot{r}$	$-1.1296 \cdot 10^{-4}$ R_J/s
$\dot{\nu}$	$-3.817 \cdot 10^{-5}$ deg/s

V. Numerical Simulations

The system was modeled using the equations of motion (Eq. 8-9) and the perturbation method (Eq. 14-18). These models were then numerically simulated using MATLAB©.

A. Perturbation Iteration

The first method of modeling the system is to iterate Eq. 14-18 with specified initial conditions and a fixed time-step such that:

$$t(i+1) = dt + t(i)$$

$$a(i+1) = \dot{a}(i, \nu(i))\, dt + a(i)$$

$$e(i+1) = \dot{e}(i, \nu(i))\, dt + e(i)$$

$$\omega(i+1) = \dot{\omega}(i, \nu(i))\, dt + \omega(i)$$

$$\theta(i+1) = \dot{\theta}(i, \nu(i))\, dt + \theta(i)$$

$$\nu(i+1) = \theta(i+1) - \omega(i+1)$$

B. Equation of Motion Integration

This portion of the simulation uses a fourth order Runge-Kutta integrator to solve the set of four first order coupled equations of motion. The algorithm uses an adaptive time step and was set to maintain a relative and absolute tolerance in meters that did not exceed $1 \cdot 10^{-3}$ and usually was set to $1 \cdot 10^{-7}$.

C. Comparison

Since the perturbation equations are clearest for an elliptical orbit, we created arbitrary initial conditions (Table 3) to compare the two methods (iteration with a 60 second time step and integration with $1 \cdot 10^{-7}$ meter tolerance).

Figure 3 gives the time evolution of the semi-major axis and eccentricity for the two methods, with integration in blue and perturbation in red points. After three orbits, the resulting semi-major axes were within 2% and the eccentricities were within 14%. Figure 4 shows a time-history plot of the two methods. Note that these points are not indicative of the time step. For sufficiently small time steps and small charges, this linearized system can model the fourth order EOM system relatively well. One could decrease this time step for improved results, but the main advantage of reduced computation time would be sacrificed.

Table 3. Initial Conditions for Simulation

a	10 R_J
e	0.65
ν	180 deg

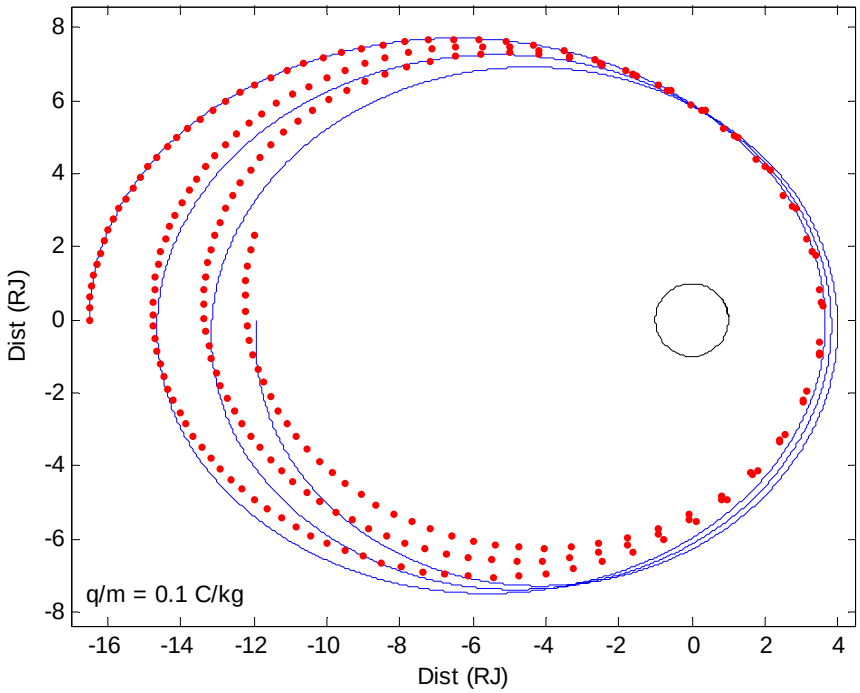

Figure 3. Orbital evolution for a constant charge craft.

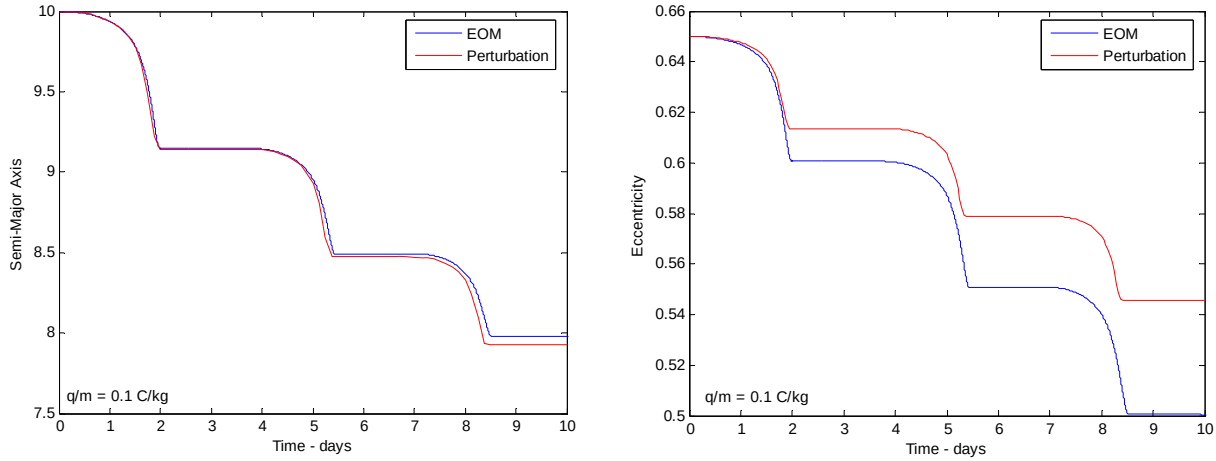

Figure 4. Orbital element evolution for a constant charged craft.

VI. Charge Control Laws

On review of the Lorentz force (Eq. 1), it is clear that the satellite will decrease energy and momentum most efficiently if it is in a retrograde approach. This sets the $\dot{\theta}$ term negative, since Jupiter has a positive ($\hat{z}$) angular momentum vector. The B_0 term is negative because Jupiter's magnetic field points from the geographic north to south pole, following the positive $\hat{\phi}$ direction.

A. Constant Charge

If the charge is set to be constant positive, the results are interesting. The satellite sheds energy and momentum as it approaches perijove, where the radial velocity vector changes direction (and thus sign). As the satellite continues, it accelerates due to the opposite net sign of its approach. The resulting time-histories for a range of charges are shown below in Fig. 5. The key feature to note is that a satellite will never be captured from a parabolic orbit if its charge is not actuated. The minimum change (q/m = 0) is by definition an escape trajectory and increasing charge leads to increasing eccentricities. This is further shown through the plot of the energy over time for the 0.4 C/kg case (Fig 6). The energy will only continue to increase, since it cannot change the sign of its velocity.

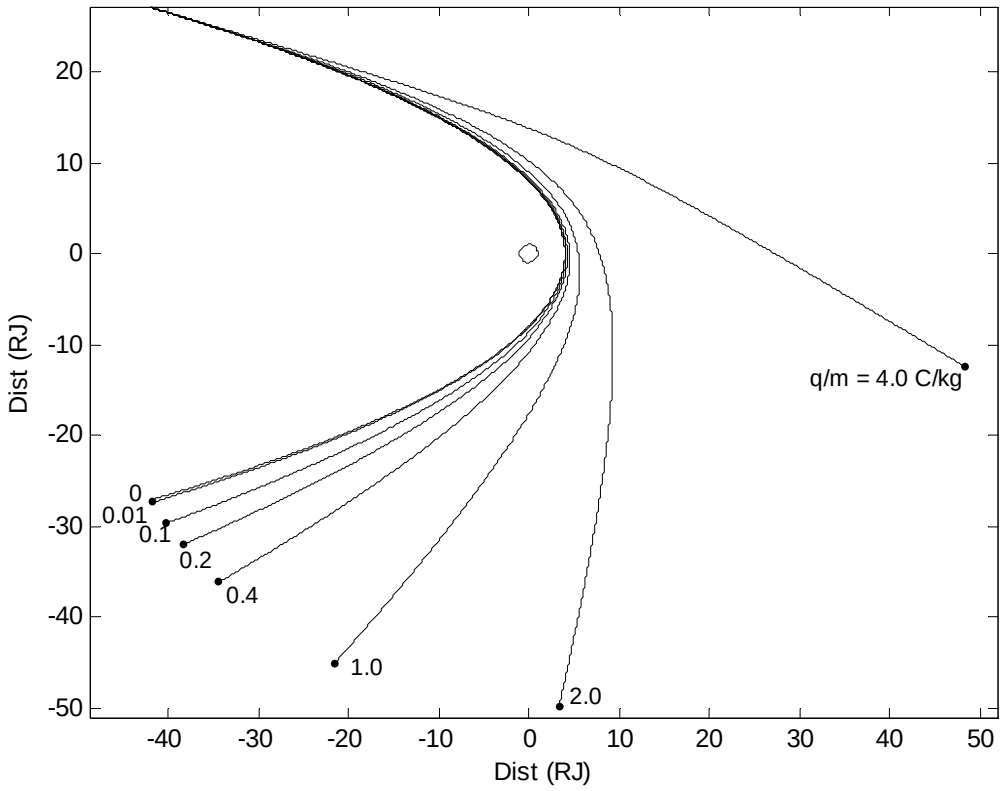

Figure 5. Constant charge time-histories.

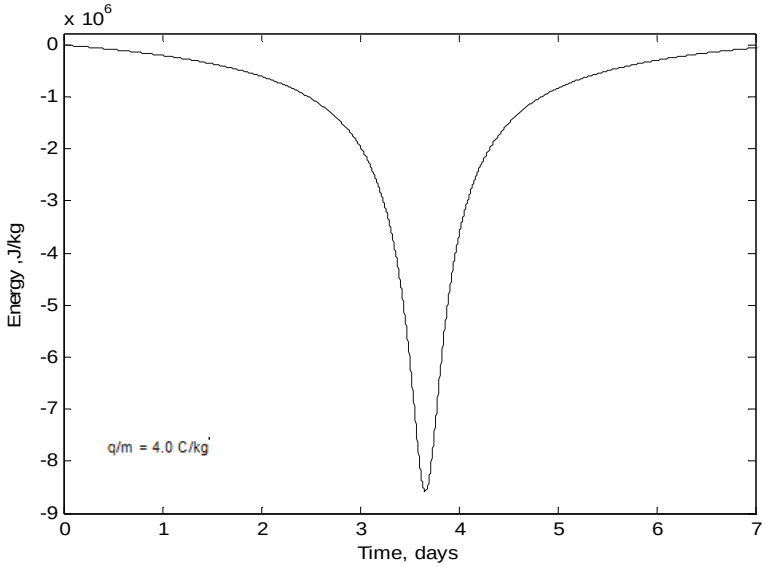

Figure 6. Energy over time for constant charge craft

B. Alternating Charge Control

Based on the previous observations, the ideal charge control would change signs as the satellite rounded the perijove. This would cause the satellite to continuously shed energy and enter a captured state. Figure 8 shows such a simulation for a charge-to-mass ratio of only 0.2 C/kg. Note that it is symmetric about the initial line of nodes, indicating a constant argument of perigee. It also demonstrates the strong reduction in elemental change as the eccentricity decreases, as illustrated first in Fig. 2.

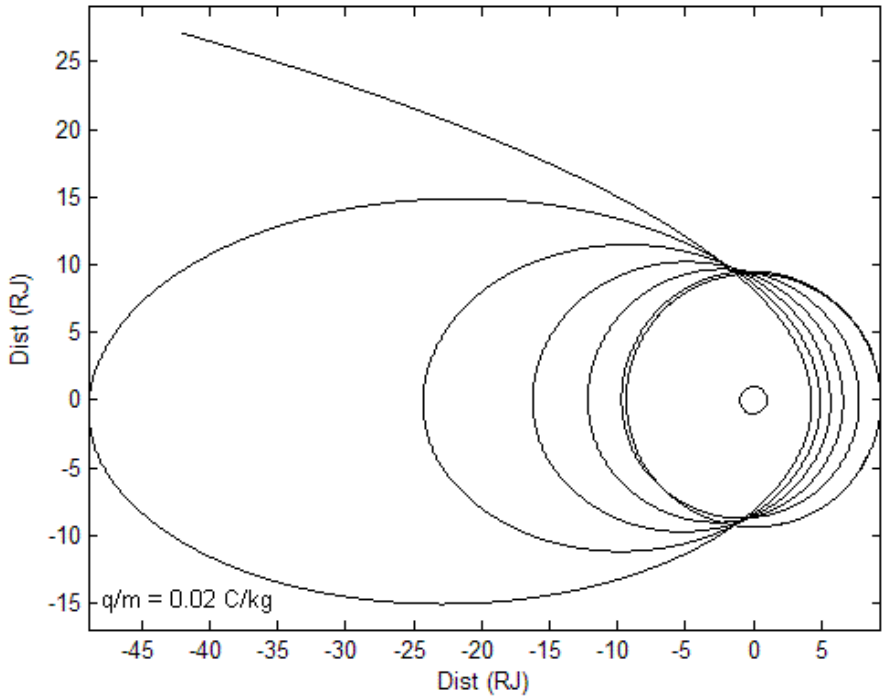

Figure 7. Time-history for alternating charged craft.

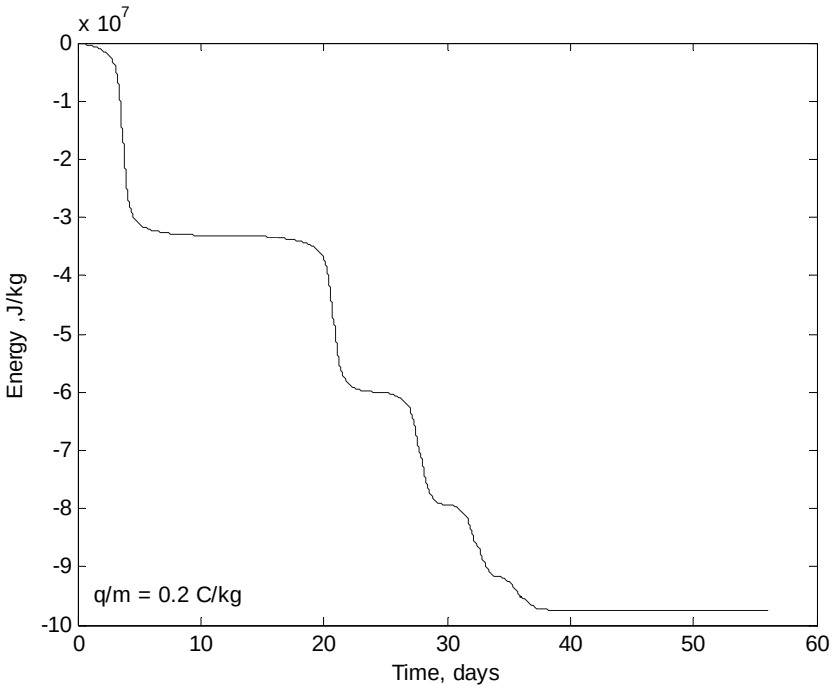

Figure 8. Energy over time for alternating charge craft

C. Bang-Bang Charge Control

The "bang-bang" charge control method, based on Hamilton-Jacobi-Bellman optimization, uses the maximum control effort throughout the interval of operation-- in this case, half of the orbit.[8] It is not optimally efficient in terms of power, in that it maintains a charge even when the Lorentz force is insignificant (for example, near apojove in a highly eccentric orbit). However, it is optimal in terms of time, in that it achieves maximum orbital evolution in a given time period.

This system is the most realizable because it requires charging in only direction (eg. expelling electrons). Figure 9 shows some interesting sample cases using this configuration over one orbit. The charge is applied while the radius is decreasing (approaching the perijove) and removed while increasing (approaching apojove). The final points in the four cases show the apojove should the charge remain removed, and correspond to three of the Jovian moons.

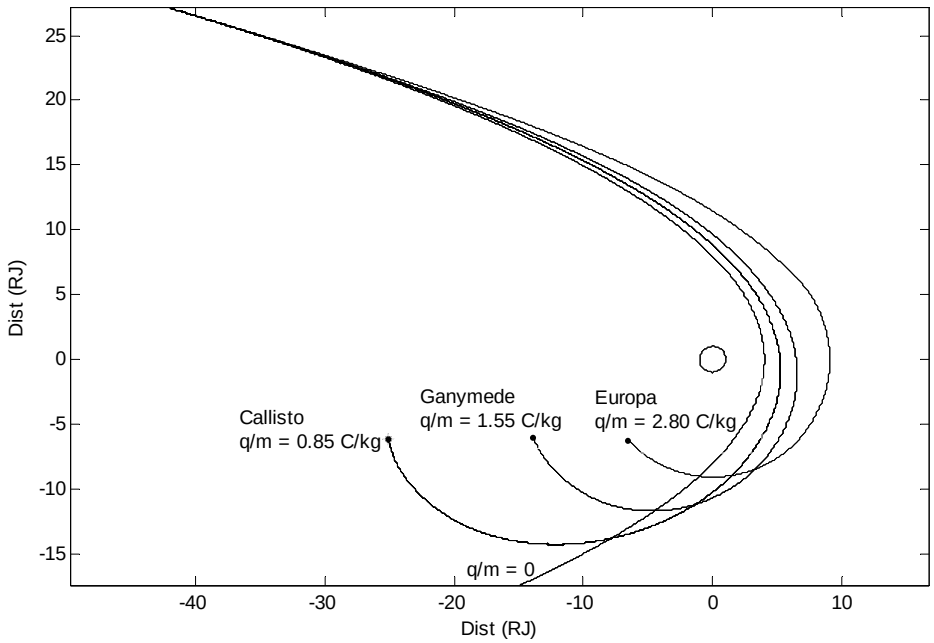

Figure 10. Time-history for various Bang-Bang charges that correspond to Jovian moons– 1 Orbit

Over a three year time span, a potentially realizable charge of only 0.05 C/kg is shown capture a satellite to Europa's orbit ($a \approx 9.3$ R_J, $e \approx 0.009$). The orbit evolution is shown in Fig. 11, and the corresponding plots of eccentricity and semi-major axis follow in Fig. 12 and 13 respectively. Admittedly, this time history is not realizable since it exceeds the bounds of the middle magnetic field range.

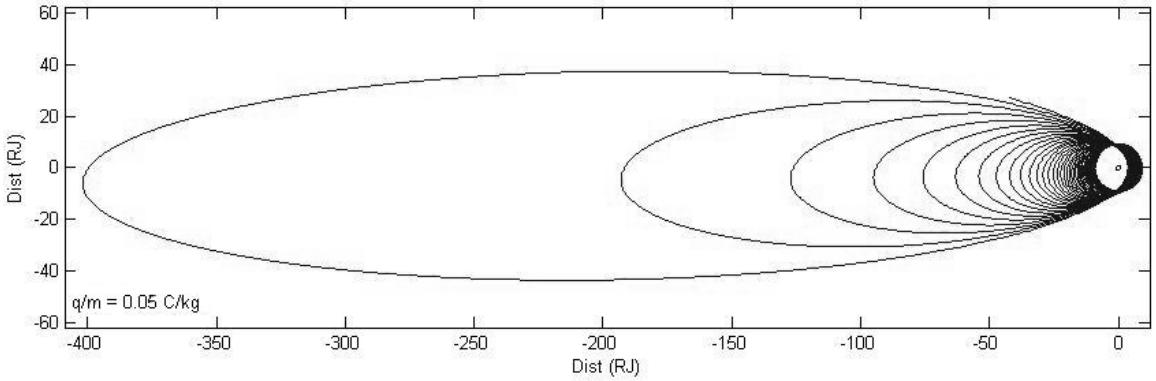

Figure 11. 3-Year Time-history of Jovian Capture to Europa

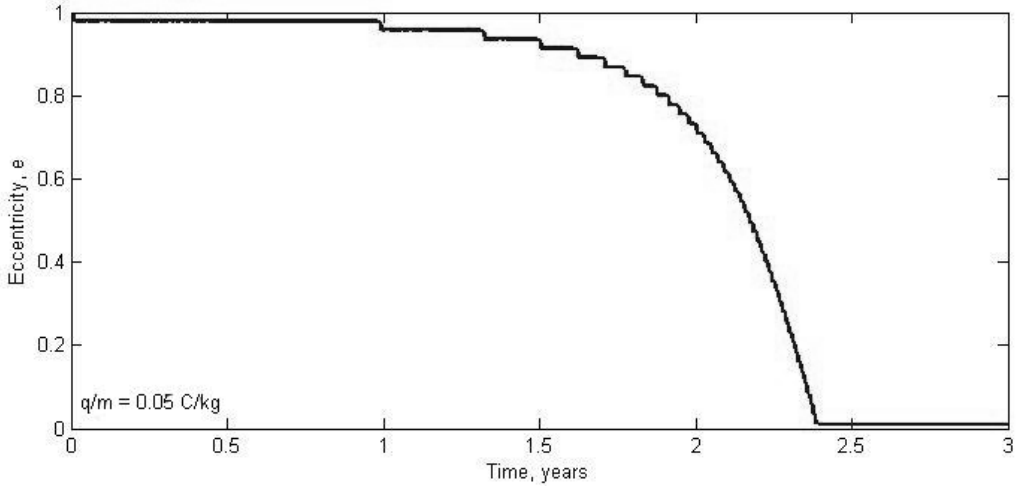

Figure 12. 3-Year time-history of eccentricity in Jovian capture to Europa

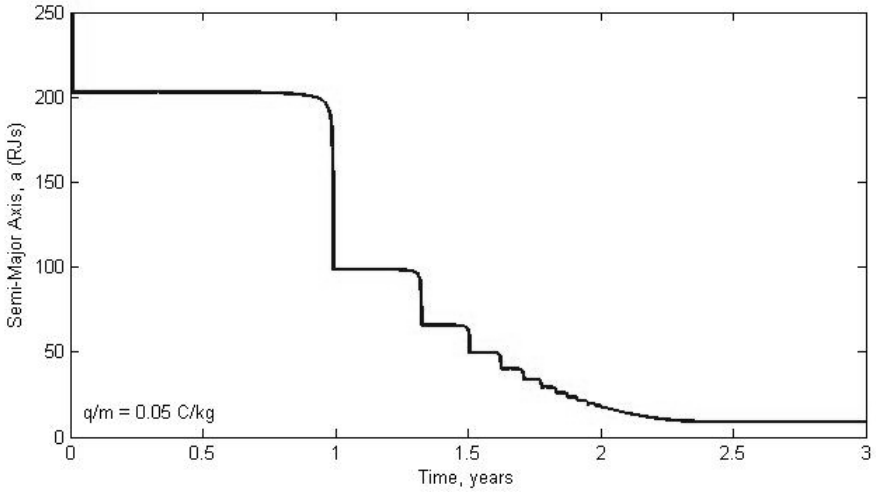

Figure 13. 3-Yr time-history of semi-major axis in Jovian capture to Europa

VII. Approach Conditions

Using the half-orbit approximations and the iterating perturbation method, we have identified a range of potential capture conditions for a given charge-to-mass ratio using a Bang-Bang charge control. At high charges and close orbits, the energy removed from the satellite directs the satellite into a collision course with Jupiter. At lower charge-to-mass ratios, the satellite requires an unreasonable amount of time to capture. With these requirements and the perturbation methods, we generated Fig. 14 which offers a range of initial semi-major axes and eccentricities that will capture a satellite of a given charge-to-mass ratio within a three year period. The upper dotted contour represents this three year time constraint. The lower solid line and charge contours represent the point at which the satellite will crash on the first orbit. The center vertical line is the parabolic condition that this simulation considers.

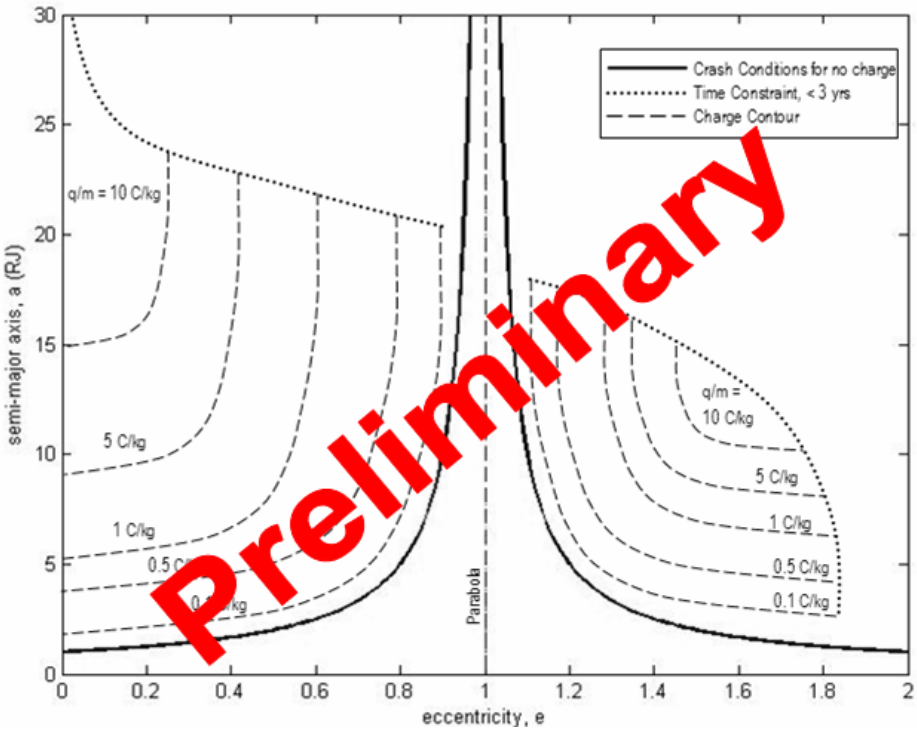

Figure 14. Preliminary investigation of successful orbit insertions for capture

VIII. Conclusions

Though a negligible perturbation for typical satellites, we show that atypical charges allow for significant energy and momentum transfer via the Lorentz force. This study evaluates the effectiveness of this finding for the case of a Jovian capture. The models indicate that the Lorentz force is indeed capable of transferring enough energy to circularize the orbit to a useful location, specifically for the potentially realizable case of a charge on the order of centicoulombs per kilogram charge modulated in a bang-bang fashion over the course of three years. This study has successfully evaluated this novel means of propellantless propulsion and justifies future research.

Acknowledgments

This work was supported in part by the NASA Institute for Advanced Concepts.

References

[1] Peck, M.A., "Prospects and Challenges of Lorentz-Augmented Orbits," *Proceedings of the AIAA Guidance, Navigation, and Control Conference*, August 2005.

[2] Schaffer, L. and Burns, J. A., "The Dynamics of Weakly Charged Dust: Motion Through Jupiter's Gravitational and Magnetic Fields," Journal of Geophysical Research, Vol. 92, 1987, pp. 2264–2280.

[3] Schaffer, L. and Burns, J. A., "Charged Dust in Planetary Magnetospheres: Hamiltonian Dynamics and Numerical Simulations for Highly Charged Grains," Journal of Geophysical Research, Vol. 99, 1994, pp. 17211–17223.

[4] Bagenal, Fran, Timothy E. Dowling, and William B. McKinnon, *Jupiter, The Planet, Satellites and Magnetosphere,* Cambridge University Press, Cambridge 2004.

[5] Hill, T.W., A.J. Dessler, and C.K. Goertz, "Magnetospheric Models," *Physics of the Jovian Magnetosphere*. Cambridge University Press, Cambridge 2002.

[6] Acuña, Mario H., Kenneth W. Behannon, and J.E.P. Connerney, "Jupiter's Magnetic Field and Magnetosphere," *Physics of the Jovian Magnetosphere*, Cambridge University Press, Cambridge 2002.

[7] Streetman, Brett and Mason Peck, "Synchronous Orbits and Disturbance Rejection Using the Geomagnetic Lorentz Force" *Proceedings of the AIAA Guidance, Navigation, and Control Conference*, August 2006. (Submitted for Publication)

[8] Kirk, Donald E. Optimal Control Theory, An Introduction, Dover Publications, Mineola, New York, 1998, pp. 246-247